MyD88 inhibition amplifies dendritic cell capacity to promote pancreatic carcinogenesis via Th2 cells

Atsuo Ochi,[1] Andrew H. Nguyen,[2] Andrea S. Bedrosian,[1] Harry M. Mushlin,[2] Saman Zarbakhsh,[1] Rocky Barilla,[1] Constantinos P. Zambirinis,[1] Nina C. Fallon,[1] Adeel Rehman,[1] Yuliya Pylayeva-Gupta,[3] Sana Badar,[1] Cristina H. Hajdu,[4] Alan B. Frey,[2] Dafna Bar-Sagi,[3] and George Miller[1,2]

[1]Department of Surgery, [2]Department of Cell Biology, [3]Department of Biochemistry and Molecular Pharmacology, and [4]Department of Pathology, New York University School of Medicine, New York, NY 10016

The transition of chronic pancreatic fibroinflammatory disease to neoplasia is a primary example of the paradigm linking inflammation to carcinogenesis. However, the cellular and molecular mediators bridging these entities are not well understood. Because TLR4 ligation can exacerbate pancreatic inflammation, we postulated that TLR4 activation drives pancreatic carcinogenesis. In this study, we show that lipopolysaccharide accelerates pancreatic tumorigenesis, whereas TLR4 inhibition is protective. Furthermore, blockade of the MyD88-independent TRIF pathway is protective against pancreatic cancer, whereas blockade of the MyD88-dependent pathway surprisingly exacerbates pancreatic inflammation and malignant progression. The protumorigenic and fibroinflammatory effects of MyD88 inhibition are mediated by dendritic cells (DCs), which induce pancreatic antigen–restricted Th2-deviated CD4+ T cells and promote the transition from pancreatitis to carcinoma. Our data implicate a primary role for DCs in pancreatic carcinogenesis and illustrate divergent pathways in which blockade of TLR4 signaling via TRIF is protective against pancreatic cancer and, conversely, MyD88 inhibition exacerbates pancreatic inflammation and neoplastic transformation by augmenting the DC–Th2 axis.

CORRESPONDENCE
George Miller:
george.miller@nyumc.org

Abbreviations used: HPF, high-powered field; MAP, mitogen-activated protein; PanIN, pancreatic intraepithelial neoplasia; PDEC, pancreatic ductal epithelial cell; Poly I:C, polyinosinic:polycytidylic acid.

Chronic pancreatitis is a fibroinflammatory disorder characterized by irreversible pancreatic destruction leading to both exocrine and endocrine organ failure. The hallmark of chronic pancreatitis is repeated cyclical fibroinflammatory responses to a primary insult such as alcoholic injury (Braganza et al., 2011). Intrapancreatic inflammation requires the activation of transcription factors, including NF-κB and AP-1 which can be induced by the RANK ligand and TNF (Vaquero et al., 2001). However, the precise cellular and biochemical mediators in chronic pancreatitis are uncertain.

An even more interesting feature of fibroinflammatory pancreatic disease is the observation that chronic pancreatitis is the leading risk factor for the development of pancreatic cancer. Epidemiological studies suggest that the incidence of pancreatic carcinoma in individuals suffering from chronic pancreatitis ranges between 1.4 and 2.7% (Ammann et al., 1984; Lankisch et al., 1993). Overall, individuals with chronic pancreatitis have a 16-fold greater lifetime risk of developing pancreatic adenocarcinoma than the general population (Jura et al., 2005). As such, the transition of chronic pancreatitis to pancreatic carcinoma represents an exemplary clinical example of the paradigm of chronic inflammation degenerating into neoplasia. Although the cellular and biochemical links between benign and malignant pancreatic disease remain poorly understood, a distinct feature of pancreatic cancer, and a commonality with chronic pancreatitis, is the extensive fibroinflammatory stroma surrounding the transformed ductal epithelial cells (Ricci et al., 2005). This suggests that the

A. Ochi and A.H. Nguyen contributed equally to this paper.

The Rockefeller University Press $30.00
J. Exp. Med. 2012 Vol. 209 No. 9 1671-1687
www.jem.org/cgi/doi/10.1084/jem.20111706

The Journal of Experimental Medicine

inflammatory stroma may have a causative role in the neoplastic transformation of chronic pancreatitis.

DCs have recently emerged as important mediators of organ-specific fibroinflammatory disease. DCs are reported to be critical to toxin-induced pulmonary inflammation and the resulting interstitial pulmonary fibrosis (Bantsimba-Malanda et al., 2010). Our recent work in the study of liver disease identified DCs as important in modulating acute and chronic inflammation after hepatic insult (Connolly et al., 2009, 2011). TLR4 activation can also drive inflammation, and recent work in pancreatitis demonstrated that TLR4 ligation stimulates pancreatic inflammation (Sharif et al., 2009; Ding et al., 2010; Zhou et al., 2010). Based on this, we postulated a role for both DCs and TLR4 in neoplastic transformation of the pancreas. Our data show that TLR4 ligation is required for neoplastic progression of pancreatic cancer as blockade of either TLR4 or the MyD88-independent TRIF pathway is protective by regulating fibroinflammatory stromal expansion. Conversely, blockade of MyD88 surprisingly accelerates pancreatic tumor progression by augmenting DC capacity to generate intrapancreatic inflammation via induction of Th2-deviated $CD4^+$ T cells.

RESULTS

TLR4 regulates pancreatic carcinogenesis

To determine the effects of TLR4 ligation on pancreatic tumor progression, we treated 4-wk-old p48Cre;$Kras^{G12D}$ mice with LPS and harvested pancreata 4 wk later. LPS greatly accelerated tumorigenesis as treated mice developed advanced pancreatic intraepithelial neoplasia (PanIN) lesions encased in a dense bed of fibroinflammatory stroma (Fig. 1, A–E). Conversely, saline-treated mice had grossly normal pancreata. Pancreata from LPS-treated p48Cre;$Kras^{G12D}$ mice also weighed roughly three times as much as controls (Fig. 1 B). Moreover, blockade of TLR4 in vivo protected p48Cre;$Kras^{G12D}$ mice against pancreatic tumorigenesis (Fig. 1, F and G). We postulated that the regulatory effects of TLR4 on pancreatic carcinogenesis result from modulation of inflammatory cell activation within the desmoplastic tumor stroma. To test this, we measured TLR4 expression on stromal leukocytes in normal pancreata and in pancreatic cancer. B cells, DCs, macrophages, and granulocytes each markedly increased their expression of TLR4 within the pancreatic cancer microenvironment (Fig. 1 H). Similarly, in human pancreatic cancer, there was robust expression of TLR4 on stromal leukocytes (Fig. 1 I). Moreover, we found elevated levels of TLR4 agonists (Fig. 1 J) and specific well-characterized DAMPs that bind TLR4 (Fig. 1 K) in human pancreatic duct fluid from cancer patients, suggesting there is ample substrate for TLR4 activation within the pancreatic cancer tumor microenvironment.

To definitively implicate peritumoral inflammation in mediating the effects of TLR4 activation on tumor progression, we made p48Cre;$Kras^{G12D}$ mice chimeric with $TLR4^{-/-}$ mice such that inflammatory cells within the tumor microenvironment would be deficient in TLR4 signaling, whereas neoplastic epithelial cells would have intact TLR4 signaling. For controls, we made age-matched p48Cre;$Kras^{G12D}$ mice chimeric using bone marrow derived from WT mice. Selected cohorts of chimeric mice were treated with caerulein to accelerate carcinogenesis as described previously (Carrière et al., 2009). WT chimeric p48Cre;$Kras^{G12D}$ mice treated with caerulein developed diffuse PanIN lesions, as expected. However, $TLR4^{-/-}$ chimeric p48Cre;$Kras^{G12D}$ mice were protected, exhibiting residual metaplastic ducts with cuboidal epithelia, suggesting that inflammatory cell TLR4 signaling can regulate pancreatic tumor progression (Fig. 2, A and B). Our extent of chimerism was >95% (not depicted; Bedrosian et al., 2011), and we confirmed deficient responses to LPS stimulation in $TLR4^{-/-}$ chimeric mice (Fig. 2 C). To further test whether the absence of TLR4 signaling in inflammatory cells is sufficient to retard tumor progression, we grafted WT and $TLR4^{-/-}$ mice with primary pancreatic ductal epithelial cells (PDECs) harboring oncogenic $KRas^{G12D}$, which we have shown form well-differentiated pancreatic lesions encased in a large stromal component mimicking early human pancreatic adenocarcinoma (Agbunag et al., 2006; Pylayeva-Gupta et al., 2012). Tumor growth was markedly slower in $TLR4^{-/-}$ hosts, again indicating that inflammatory cell expression of TLR4 can modulate cancer progression (Fig. 2 D). Furthermore, because TLR4 generates inflammation via NF-κB and mitogen-activated protein (MAP) kinase, as anticipated, blockade of NF-κB and MAP kinase signaling partially protected LPS-treated p48Cre;$Kras^{G12D}$ mice from accelerated carcinogenesis (not depicted).

Dichotomous effects of TRIF and MyD88 signaling interruption

To test whether effects of TLR4 activation in pancreatic cancer are primarily mediated via the MyD88-independent TRIF pathway or the MyD88-dependent pathway, we selectively blocked each mechanism in p48Cre;$Kras^{G12D}$ mice using cell-permeable inhibitors. TRIF blockade (Fig. 2 E) prevented p48Cre;$Kras^{G12D}$ mice from developing accelerated carcinogenesis after treatment with caerulein (Fig. 2 F) or LPS (not depicted). Similarly, adoptive transfer of $Kras^{G12D}$ PDECs to $TRIF^{-/-}$ mice resulted in retarded tumor growth compared with $Kras^{G12D}$ PDEC transfer to WT mice (Fig. 2 G). Consistent with its regulatory effects in the tumor microenvironment, $TRIF^{-/-}$ mice were also protected against pancreatitis (Fig. 2 H). Notably, TLR3 ligand (polyinosinic:polycytidylic acid [Poly I:C]), which also signals via TRIF, similarly accelerated carcinogenesis in p48Cre;$Kras^{G12D}$ mice (Fig. 2 I).

In contrast to the protective effects of TRIF blockade, MyD88 inhibition (Fig. 3 A) markedly accelerated pancreatic carcinogenesis (Fig. 3, B–D). In particular, whereas control p48Cre;$Kras^{G12D}$ mice treated with caerulein developed metaplastic ducts and diffuse low-grade PanIN lesions, animals treated with MyD88 inhibitory peptide developed pancreatic tumors three to four times the size of controls (Fig. 3 B). On histological examination, MyD88 blockade resulted in invasive cribriforming pancreatic adenocarcinoma which exhibited a markedly high proliferation rate and increased expression of p53 (Fig. 3 C) as well as foci of invasion as confirmed by

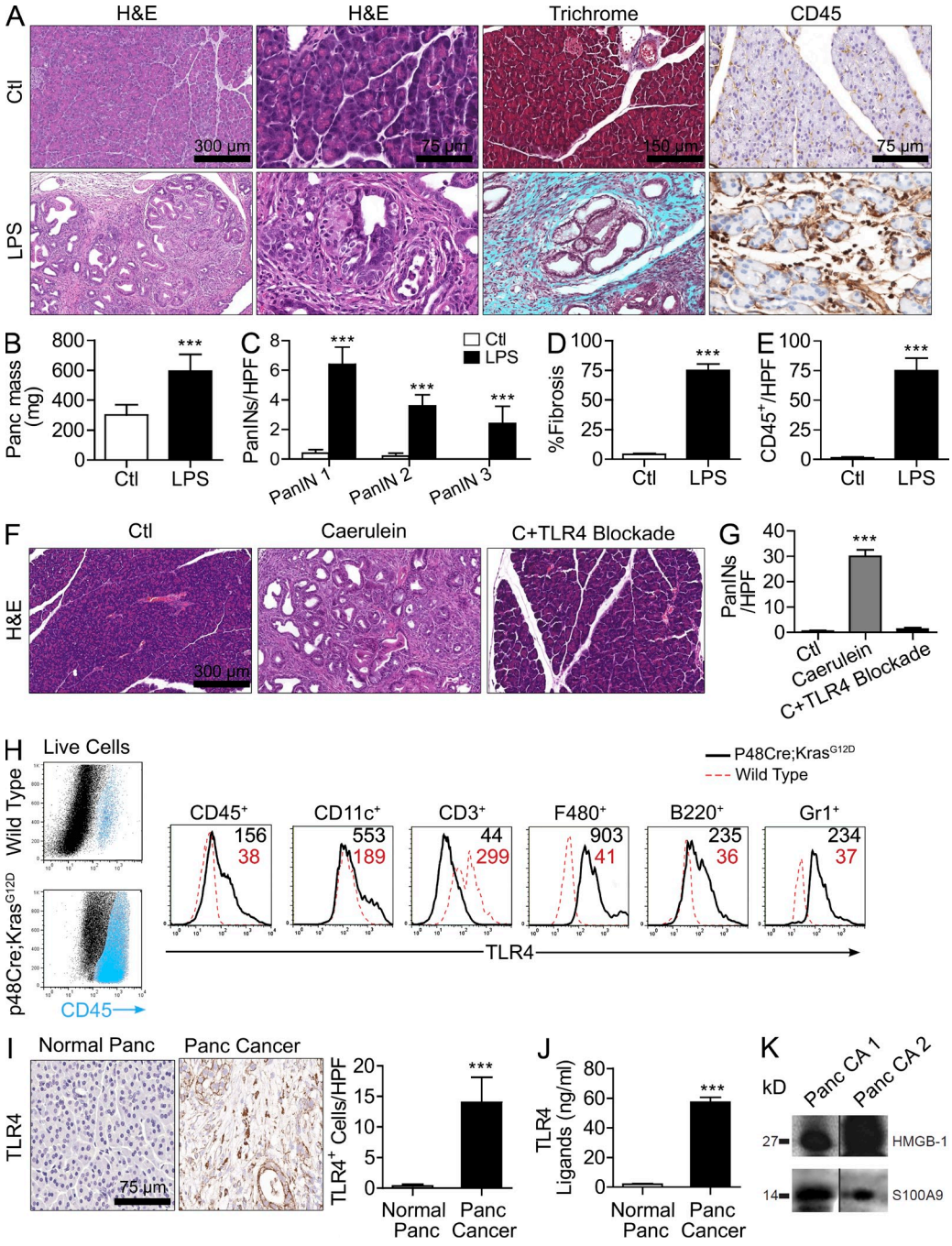

Figure 1. TLR4 signaling modulates pancreatic carcinogenesis. (A–E) 4-wk-old p48Cre;Kras^{G12D} mice were treated with saline or LPS and sacrificed at 4 wk. (A and B) Pancreata were stained with H&E, Trichrome, and CD45 (A) and weighed (B). (C–E) The presence of graded PanIN lesions (C), fibrotic area (D), and leukocytic infiltrate (E) were quantified by examining 10 high-powered fields (HPFs) per pancreas (n = 6 mice/group; ***, $P < 0.001$). (F and G) 4-wk-old p48Cre;Kras^{G12D} mice were treated with saline, caerulein, or caerulein + TLR4 inhibitor. Representative H&E-stained sections are shown, and the number of dysplastic ducts per HPF was calculated (n = 5 mice/group; ***, $P < 0.001$). (H) Live pancreatic mononuclear cells from 6-mo-old p48Cre;Kras^{G12D} or WT mice were gated and costained for CD45, CD11c, CD3, F480, B220, Gr1, and TLR4. Median fluorescence for TLR4 is shown for specific cellular subsets. Data are representative of experiments repeated three times. (I) Sections of normal human pancreas (n = 3) and human pancreatic cancer (n = 19) were stained for TLR4. Representative images are shown, and data were quantified (***, $P < 0.001$). (J) Pancreatic duct fluid was harvested at the time of surgical resection from four patients with pancreatic cancer and two patients with benign endocrine tumors and tested for TLR4 ligand levels on HEK-Blue reporter cells (***, $P < 0.001$). (K) Pancreatic ductal fluid from two patients with pancreatic carcinoma was harvested at the time of operative duct transection and analyzed for HMGB-1 and S100A9 expression by Western blotting. Error bars indicate standard error of the mean.

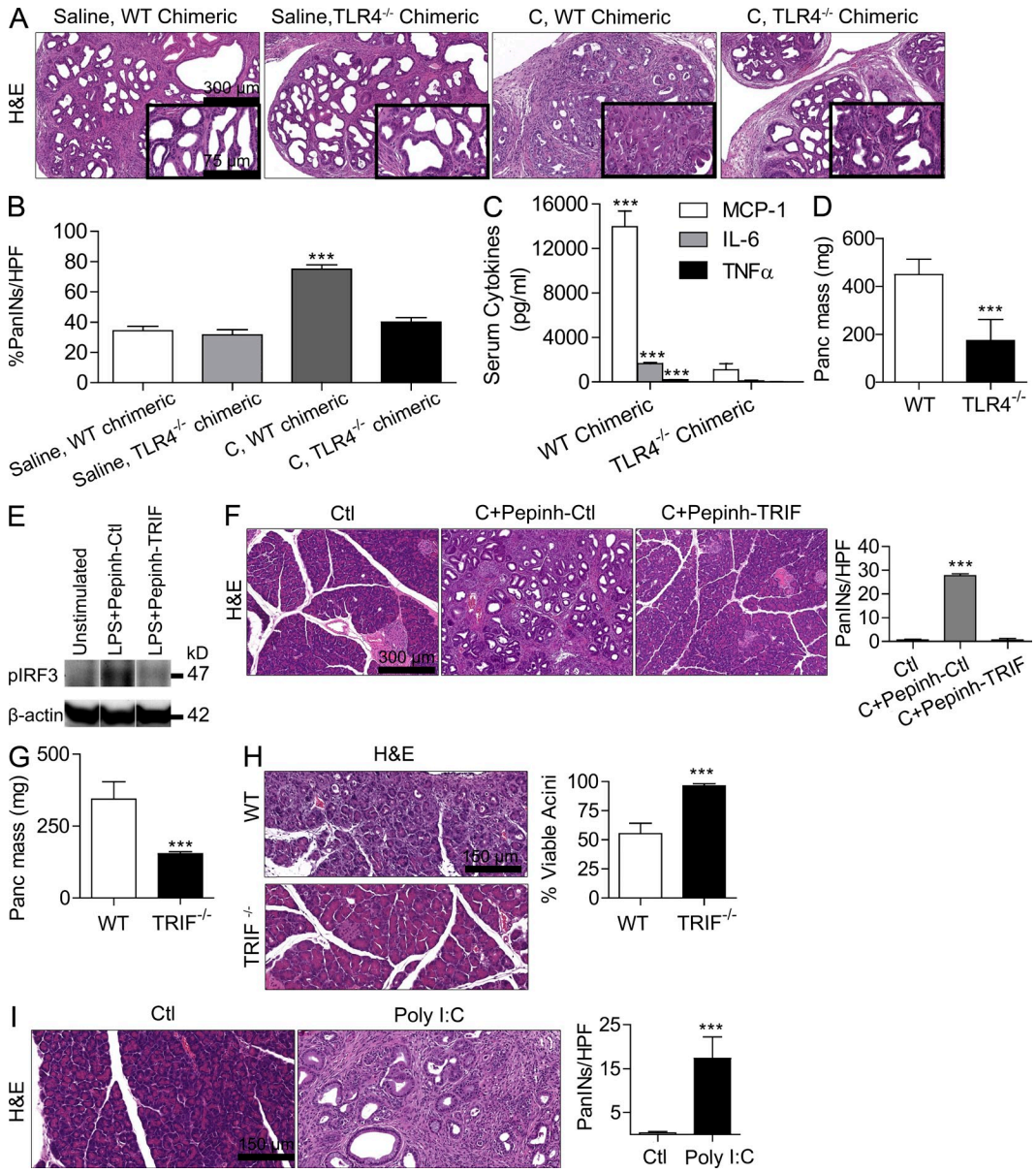

Figure 2. TLR4 regulation of pancreatic tumorigenesis and pancreatitis is mediated by stromal inflammatory cells and requires TRIF.
(A and B) p48Cre;Kras^{G12D} mice were irradiated and made chimeric by bone marrow transfer from WT or TLR4$^{-/-}$ mice. 7 wk later, mice were treated with either saline or two doses of caerulein (C). Three weeks afterward, mice were sacrificed and pancreata were assessed by H&E. The fraction of dysplastic ducts was measured (n = 5/group; ***, P < 0.001). Insets show higher magnification. (C) WT chimeric and TLR4$^{-/-}$ chimeric mice were treated with 5 µg LPS. Serum cytokine levels were measured at 6 h (***, P < 0.001). (D) WT or TLR4$^{-/-}$ mice were adoptively transferred with intrapancreatic Kras^{G12D} PDECs. Pancreata were harvested and weighted at 6 wk (n = 5 mice/group; ***, P < 0.001). (E) Raji cells were stimulated for 90 s with 1 µg/ml LPS in the presence of TRIF inhibitor (Pepinh-TRIF) or control peptide (Pepinh-Ctl). Expression of pIRF3 and β-actin was measured by Western blotting. (F) 4-wk-old p48Cre;Kras^{G12D} mice were treated with saline, caerulein + control peptide, or caerulein + TRIF inhibitor. Representative H&E-stained sections are shown, and the number of dysplastic ducts per HPF was calculated (n = 5 mice/group; ***, P < 0.001). (G) WT or TRIF$^{-/-}$ mice were adoptively transferred with intrapancreatic Kras^{G12D} PDECs. Pancreata were harvested and weighted at 6 wk (n = 4–5 mice/group; ***, P < 0.001). (H) Acute pancreatitis was induced using caerulein in WT or TRIF$^{-/-}$ mice. The fraction of viable acini was calculated (n = 4 mice/group; ***, P < 0.001). (I) 4-wk-old p48Cre;Kras^{G12D} mice were treated with saline or Poly I:C before sacrifice 4 wk later. Representative H&E-stained sections are shown, and the number of PanIN lesions per HPF was quantified (n = 4 mice/group; ***, P < 0.001). Error bars indicate standard error of the mean.

positive staining for CK19 outside of ductal structures (Fig. 3 D). Gene sequencing revealed no somatic mutation in p53 (not depicted). To confirm that the tumor-promoting effects of MyD88 inhibition occur within inflammatory cells, we made p48Cre;Kras^{G12D} mice chimeric with MyD88$^{-/-}$ bone marrow before caerulein treatment. Controls were made chimeric using WT bone marrow. MyD88$^{-/-}$ chimeric mice developed more extensive fibroinflammatory replacement of their

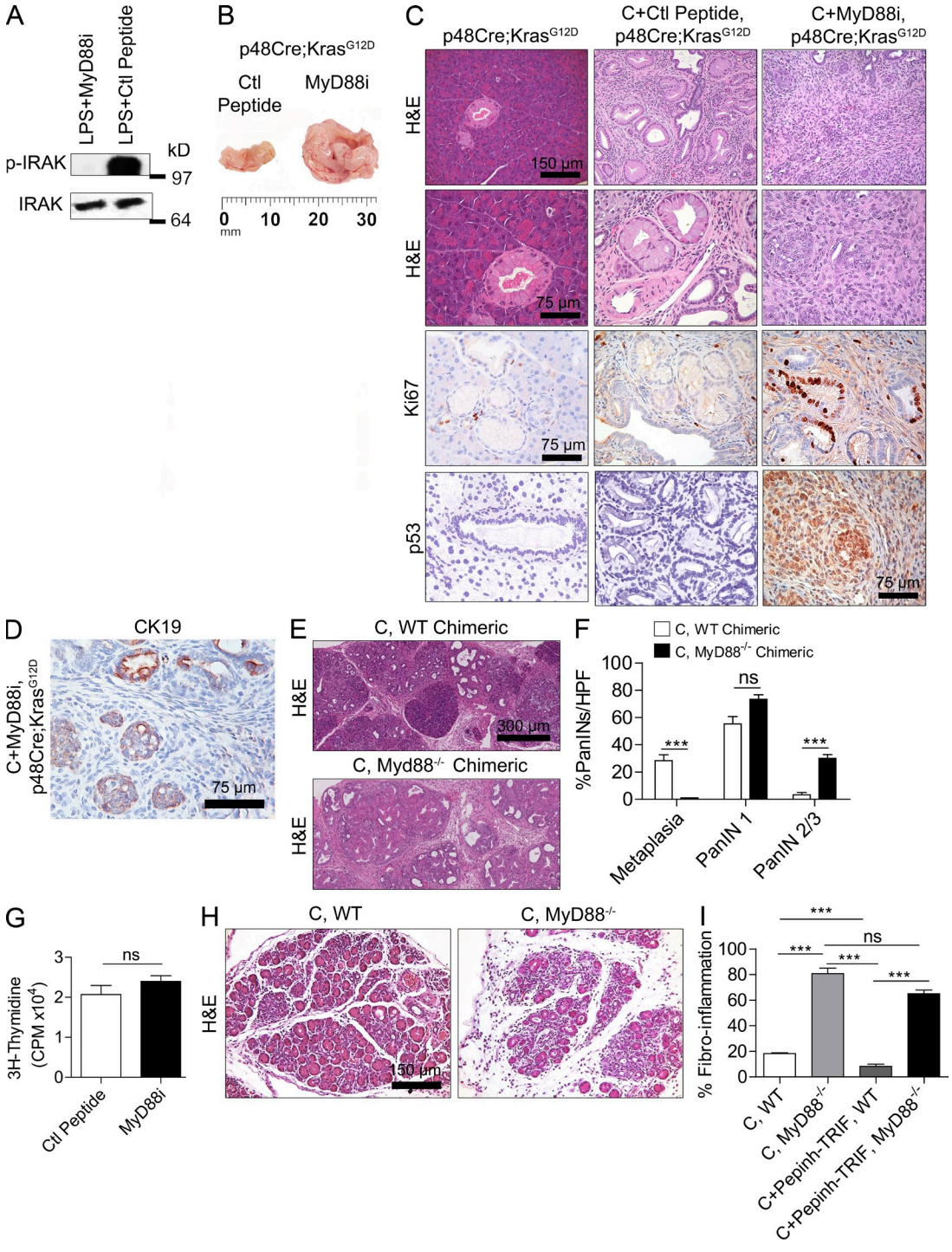

Figure 3. MyD88 blockade accelerates malignant transformation and stromal inflammation. (A) Mice were treated with LPS and MyD88 inhibitory peptide (MyD88i) or control peptide. At 6 h, pancreata were assayed for expression of IRAK and p-IRAK. (B–D) p48Cre;Kras^{G12D} mice were treated with caerulein for 2 d to accelerate carcinogenesis before sacrifice 3 wk later. In addition, mice were administered either MyD88 inhibitory peptide or control peptide. (B) Tumor size was recorded. (C and D) Paraffin-embedded pancreatic sections were stained using H&E and Ki67 and using mAbs directed against p53 (C) and CK19 (D) an epithelial cell marker (n = 6 mice/group). (E and F) WT chimeric and MyD88$^{-/-}$ chimeric p48Cre;Kras^{G12D} mice were treated with caerulein and sacrificed at 3 wk. The fraction of metaplastic ducts and PanIN lesions was quantified (n = 4–6 mice/group; ***, P < 0.001). (G) Kras^{G12D} PDECs were cultured with MyD88 inhibitory peptide or control peptide. Cells were pulsed with [^{3}H]thymidine for 20 h, and its incorporation was measured. (H and I) MyD88$^{-/-}$ and WT mice were challenged with caerulein alone or caerulein + TRIF inhibitor or control peptide for 3 wk. Fibro-inflammatory changes were quantified (n = 4–6 mice/group; ***, P < 0.001). Error bars indicate standard error of the mean.

acinar architecture and advanced PanIN lesions compared with WT chimerics (Fig. 3, E and F). Furthermore, MyD88 inhibition did not appear to have direct effects on epithelial cells as $Kras^{G12D}$ PDECs did not exhibit altered viability (not depicted) or an accelerated proliferative rate in vitro in response to MyD88 inhibitor (Fig. 3 G). In consort with these findings, which suggest that MyD88 inhibition activates peritumoral inflammatory cells compared with WT mice subject to pancreatitis, $MyD88^{-/-}$ mice developed exacerbated pancreatic fibroinflammation, even in the context of TRIF inhibition (Fig. 3, H and I). Collectively, these data show that blockade of the MyD88-dependent pathway and the MyD88-indepedant TRIF pathway have distinctly opposite effects in benign and malignant pancreatic disease.

DCs and $CD4^+$ T cells mediate effects of MyD88 inhibition in pancreatic disease

Because Th2-deviated $CD4^+$ T cells have been implicated in pancreatic inflammation (Demols et al., 2000; Oiva et al., 2010) and MyD88 inhibition skews DC-mediated T cell differentiation toward the Th2 phenotype (Kaisho et al., 2002; Kapsenberg, 2003; Chen et al., 2010), we postulated that DCs may be the central cellular entity responsible for the exacerbated pancreatic inflammation and tumorigenesis associated with MyD88 inhibition by inducing effector Th2-deviated $CD4^+$ T cells. To directly test whether DCs are responsible for exacerbated pancreatic disease in MyD88-deficient mice, we generated CD11c-Cre MyD88 $Floxed^{+/+}$ mice, which are deficient in MyD88 signaling in $CD11c^+$ DCs (Hou et al., 2008). We found minimal CD11c expression in other intrapancreatic leukocytes subsets (not depicted). CD11c-Cre MyD88 $Floxed^{+/+}$ mice were then challenged with caerulein to induce pancreatitis. In consort with our hypothesis, CD11c-Cre MyD88 $Floxed^{+/+}$ mice experienced exacerbated pancreatic fibroinflammatory disease compared with controls (Figs. 4 A) and to a similar extent as pan-MyD88–deficient animals (not depicted). To determine whether MyD88 inhibition within DCs is also associated with accelerated pancreatic carcinogenesis, we made p48Cre;$Kras^{G12D}$ mice chimeric using bone marrow from either WT or CD11c-Cre MyD88 $Floxed^{+/+}$ mice followed by administration of caerulein 7 wk later. CD11c-Cre MyD88 $Floxed^{+/+}$ chimeric p48Cre;$Kras^{G12D}$ mice experienced accelerated cancer progression when compared with WT chimeric controls (Fig. 4 B).

Consistent with our hypothesis, we found that $CD4^+$ T cell recruitment was increased >20-fold in pancreata of caerulein-treated $MyD88^{-/-}$ mice compared with WT controls (not depicted) and MyD88 inhibition resulted in a significant Th2 deviation in both benign and malignant pancreatic disease (Fig. 4 C). Moreover, $CD4^+$ T cell depletion (Miller et al., 2003) rescued mice from the exacerbated fibroinflammation (not depicted) and accelerated cancer progression (Fig. 4 D) associated with MyD88 inhibition. However, $CD4^+$ T cell depletion did not rescue p48Cre;$Kras^{G12D}$ mice with intact MyD88 signaling capacity (Fig. 4 D). Collectively, the aforementioned observations indicate that (a) MyD88 inhibition exclusively within DCs is sufficient to induce exacerbated pancreatic inflammation and carcinogenesis (Fig. 4, A and B) and (b) MyD88 blockade exacerbates pancreatic disease in a $CD4^+$ T cell–dependent manner (Fig. 4 D).

To directly test whether the DC–Th2 axis is central to pancreatic inflammation, before beginning caerulein challenge in WT mice, we treated mice with VAG539, which binds the DC aryl hydrocarbon receptor in vivo and prevents DC induction of antigen-restricted Th2 cells as we and others have recently shown (Hauben et al., 2008; Connolly et al., 2011). We confirmed that intrapancreatic $CD4^+$ T cells are prevented from Th2 deviation after treatment with VAG539 (Fig. 4 E). Consistent with our expectation, VAG539 markedly protected against pancreatic inflammation (Fig. 4 F).

DCs expand in chronic pancreatitis and pancreatic adenocarcinoma

To further investigate the role of DCs in chronic pancreatic inflammation and malignant transformation, we examined the prevalence of DCs in pancreatic cancer and chronic pancreatitis. The fraction and total number of DCs were markedly increased in the pancreata of p48Cre;$Kras^{G12D}$ mice compared with age-matched WT controls (Fig. 5, A–C). The surface phenotype of DCs infiltrating p48Cre;$Kras^{G12D}$ pancreata differed from controls in that they contained a large $B220^+$ plasmacytoid subset (Fig. 5 D) and an increased fraction of $CD8^+CD11^-$ lymphoid DCs (Fig. 5 E) and were highly mature, expressing elevated CD40 and CD86 (Fig. 5 E). To determine whether an intense DC infiltrate was similarly associated with human pancreatic cancer, we tested 19 human pancreatic carcinoma specimens for an array of DC markers. Consistent with our murine findings, there was a robust infiltrate of $CD123^+$ cells, characteristic of plasmacytoid DCs, in all specimens tested (Fig. 5 F). DC-$SIGN^+$ and $CD1a^+$ cells were also present but in smaller numbers (Fig. 5 F).

To investigate whether DC expansion within the pancreas was a function of neoplasia or similarly associated with benign chronic pancreatic inflammation, we examined the prevalence of DCs, outside of the context of oncogenic Kras, in caerulein-induced chronic pancreatitis in WT mice. We found that DCs accounted for 1–3% of $CD45^+$ leukocytes in normal pancreata but increased to 10–15% during chronic pancreatitis induction (Fig. 5 G). Moreover, the absolute number of pancreatic DCs increased 100-fold (Fig. 5 H). Conversely, the fraction of DCs in the spleen remained unchanged, implying a pancreas-specific expansion in chronic pancreatitis (Fig. 5 G). Collectively, these data show that a large DC infiltrate is a common feature in neoplastic and inflammatory pancreatic disease.

DCs exacerbate pancreatic fibroinflammation and ductal transformation

To directly test DC capacity to potentiate intrapancreatic inflammation via Th2 cells, we further expanded the pancreatic DC population by i.p. adoptive transfer of bone marrow–derived DCs to mice developing chronic pancreatitis. Creusot et al. (2009) reported that the plurality of bone marrow–derived

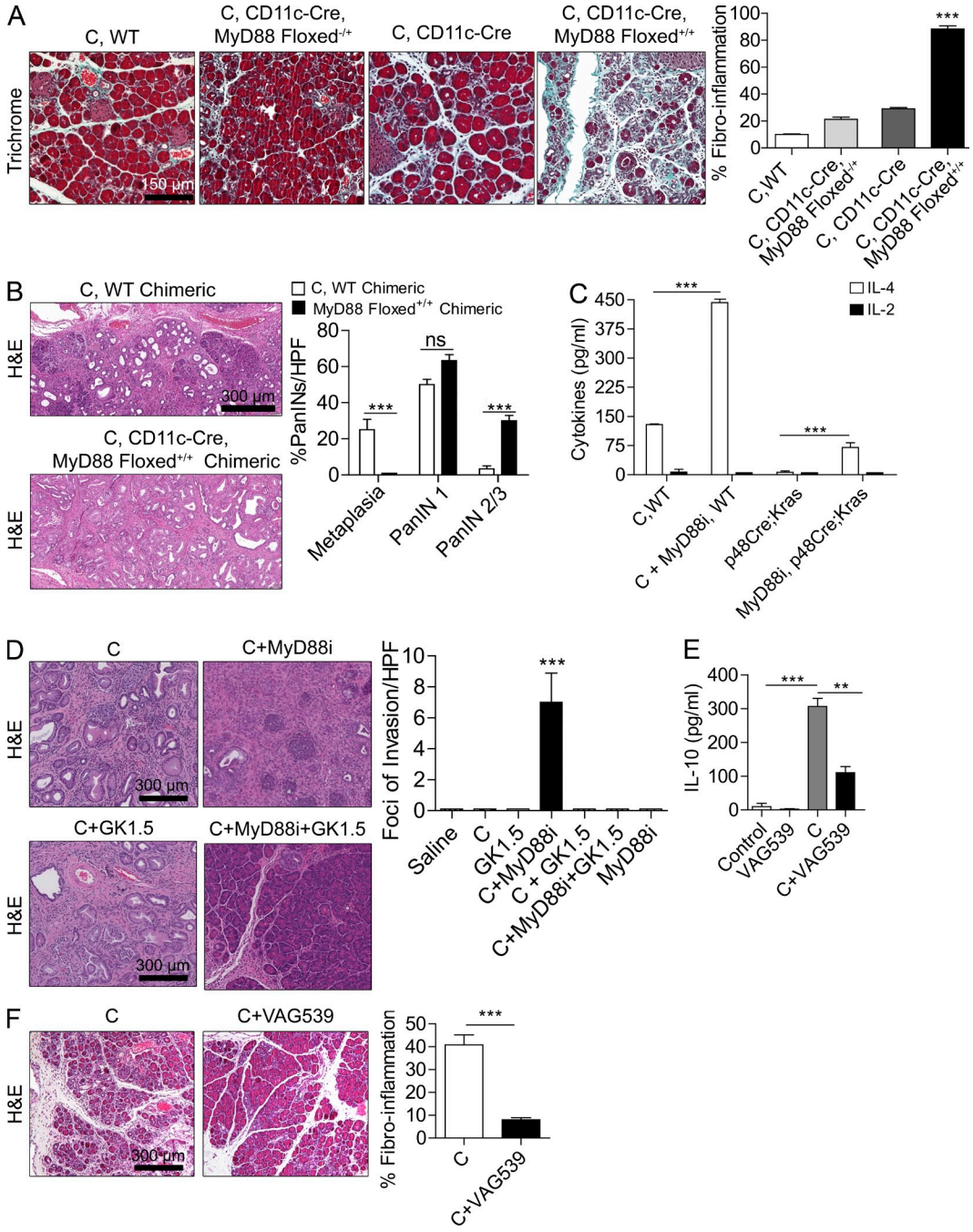

Figure 4. MyD88 blockade within DCs exacerbates pancreatic disease in a CD4⁺ T cell–dependent manner. (A) 4-wk-old CD11c-Cre MyD88 Floxed$^{+/+}$ mice and control animals were treated with caerulein (C) for 3 wk to induce chronic pancreatitis. Pancreata were examined by Trichrome staining, and the fibroinflammatory area was quantified (n = 4 mice/group; ***, P < 0.001). (B) p48Cre;Kras^{G12D} mice were made chimeric using bone marrow derived from WT or CD11c-Cre MyD88 Floxed$^{+/+}$ mice. Chimeric mice were treated with caerulein and sacrificed at 3 wk (n = 4–5/group). Representative images are shown, and the fraction of graded PanIN lesions was quantified (***, P < 0.001). (C) CD4⁺ T cells were harvested from the pancreata of p48Cre;Kras^{G12D} mice and caerulein-treated WT mice that were administered MyD88 inhibitory peptide or control peptide. IL-2 and IL-4 levels were measured in cell culture supernatant (***, P < 0.001). (D) 4-wk-old p48Cre;Kras^{G12D} mice were treated with C, C + MyD88 inhibitor, C + GK1.5 to deplete CD4 T cells, C + MyD88 inhibitor + GK1.5, or additional controls. Mice were sacrificed at 3 wk, and the foci of invasive cancer were quantified by examining 10 HPFs per mouse (n = 5 mice/group; ***, P < 0.001). (E) IL-10 was measured in cell culture supernatant from purified pancreatic CD4⁺ T cells from mice treated for 2 d with saline, VAG539, caerulein, or caerulein + VAG539 (***, P < 0.001). (F) WT mice were treated with caerulein alone or caerulein + VAG539 for 3 wk. Representative H&E-stained sections are shown (n = 4 mice/group), and fibroinflammatory changes were quantified (***, P < 0.001). Error bars indicate standard error of the mean.

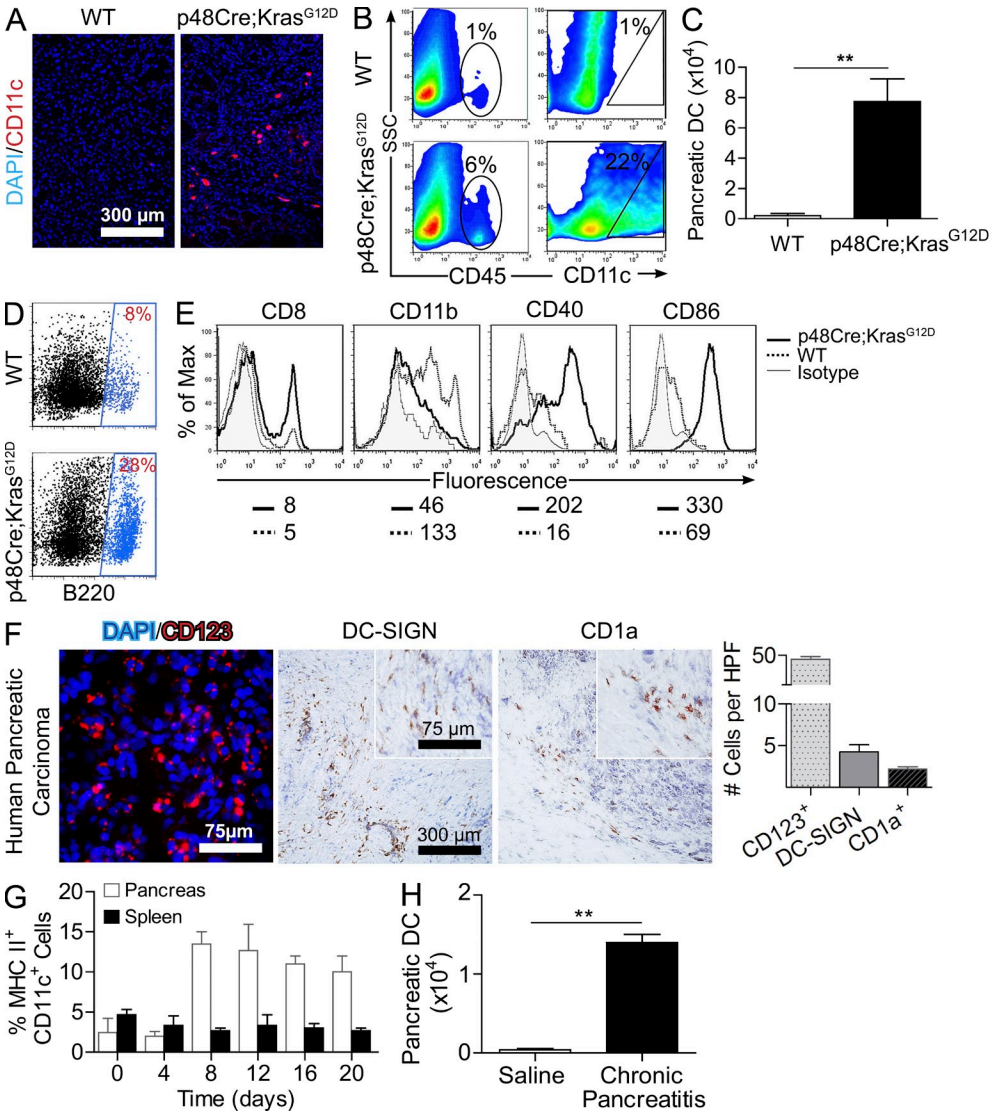

Figure 5. DCs expand in pancreatic carcinoma and chronic pancreatitis. (A) Pancreata from p48Cre;Kras^{G12D} and WT mice were examined by immunofluorescence using anti-CD11c. (B and C) In addition, the fraction of both CD45$^+$ and CD11c$^+$ leukocytes (B) and the total number of DCs (C) in pancreata of 9-mo-old p48-Cre;Kras^{G12D} and WT mice were determined by flow cytometry (**, $P < 0.01$). (D and E) DCs from the pancreata of WT and p48-Cre;Kras^{G12D} mice were further examined for B220 (D) and additional surface marker expression (E). Median fluorescence is shown below respective histograms. Experiments are representative of those repeated more than three times using a mean of three mice per group. (F) Frozen sections of human pancreatic cancer specimens were examined by immunofluorescence (CD123) and immunohistochemistry (DC-SIGN and CD1a). Insets show higher magnification. (G) The fraction of DCs among all CD45$^+$ leukocytes in both the pancreas and the spleen was measured at timed intervals during the 3-wk course of caerulein administration in WT mice (mean of four mice per data point). (H) The total number of DCs per pancreas was measured on day 21 of saline or caerulein administration in WT mice (**, $P < 0.01$). Error bars indicate standard error of the mean.

DCs migrate to the peripancreatic tissues within 24 h after adoptive transfer and remain there for at least 12 d. After 3 wk of treatment with saline (Ctl), caerulein (C), DCs, or caerulein and DCs (C+DCs), pancreata were harvested and assessed for extent of fibrosis, inflammation, and endocrine and exocrine destruction.

Mice treated with C+DCs developed distortion of their pancreatic architecture including the formation of thick fibrous bands between lobules and effacement of the intralobular space with inflammatory fibroplasia (Fig. 6, A–C). On average, >50% of the pancreatic surface area was replaced by fibroplasia in C+DC-treated mice (Fig. 6, A–C). This resulted in destruction of both the exocrine and endocrine pancreas, including a >60% reduction in acinar cell volume (Fig. 6, D and E), and a marked reduction in islet cell mass (Fig. 6 F). In consort with the latter findings, mice developed overt diabetes by 3 wk of C+DC challenge (Fig. 6 G). The severity of pancreatic exocrine destruction was exemplified by a roughly fourfold diminution in pancreatic-specific serum lipase levels in C+DC-treated mice (not depicted). Furthermore, DC

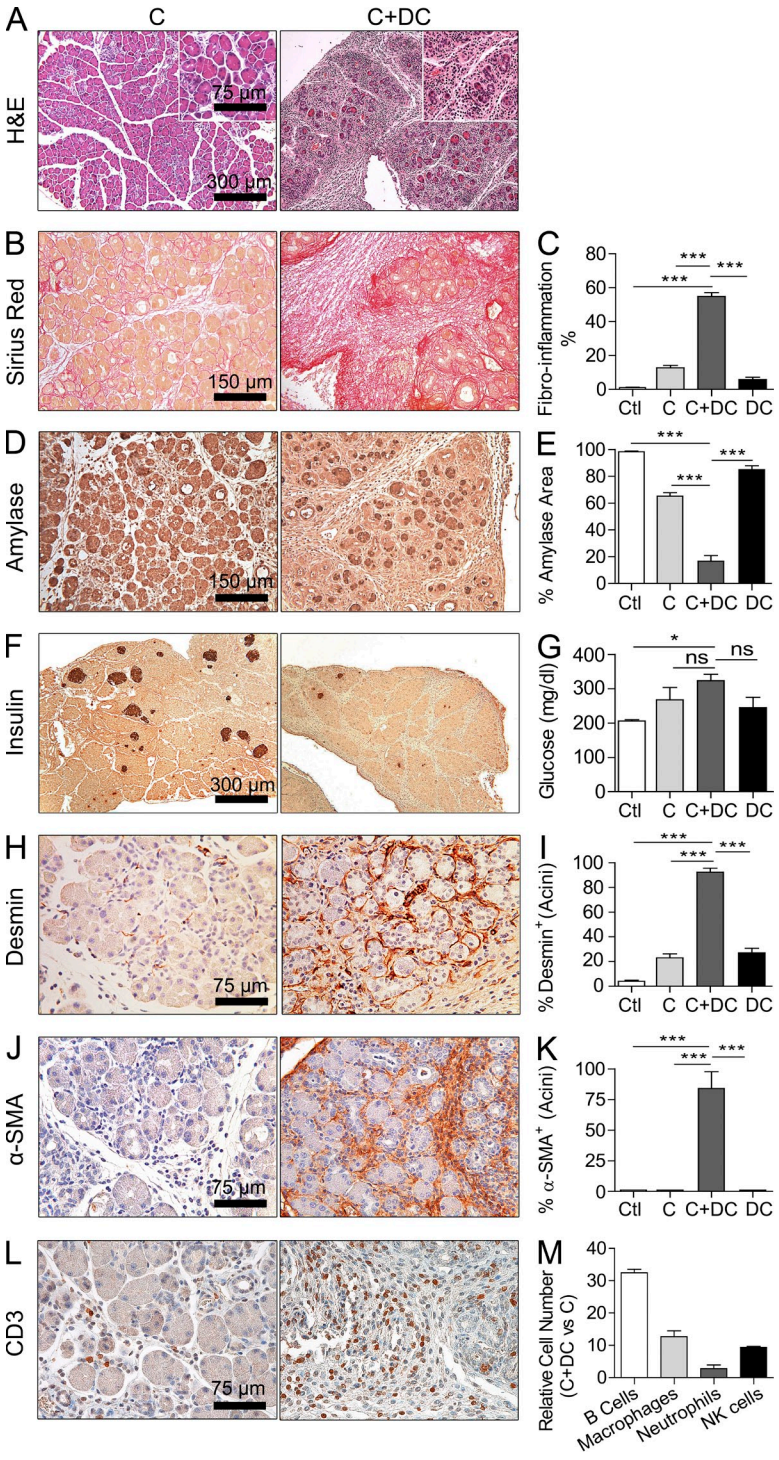

Figure 6. DCs exacerbate pancreatic fibroinflammation. WT mice were treated with saline, C alone, DCs alone, or C+DCs. (A–C) Paraffin-embedded sections of pancreata were stained with H&E (A) and Picric acid–Sirius red (B), and the fibroinflammatory area per mouse pancreas was calculated for all treatment groups (C). Insets show higher magnification. (D–G) Pancreata were also stained using mAbs directed against amylase (D and E) and insulin (F), and serum glucose (G) levels were calculated. (H–L) Similarly, pancreata were stained using mAbs directed against desmin (H and I), α-SMA (J and K), and CD3 (L). (M) Using flow cytometry, the relative number of intrapancreatic B cells, macrophages, neutrophils, and NK cells in chronic pancreatitis in the context of exogenous DCs expansion was calculated (n = 8–10 mice/group; *, $P < 0.05$; ***, $P < 0.001$). Error bars indicate standard error of the mean.

transfer in chronic pancreatitis resulted in pancreatic stellate cell activation in vivo as indicated by increased expression of periacinar desmin (Fig. 6, H and I) and α-SMA (Fig. 6, J and K) in pancreata of C+DC-treated mice. Pancreatic stellate cell activation is necessary for pancreatic fibrosis and neoplastic progression (Omary et al., 2007; Masamune et al., 2009). In addition, overexpansion of DCs in the context of pancreatitis resulted in the recruitment of a robust immune infiltrate. In particular, there was an increased T cell infiltrate (Fig. 6 L) as well as a substantial increase in B cell, macrophage, neutrophil, and NK cell populations (Fig. 6 M). The effects of C+DC treatment were pancreas specific as there was no effacement of the kidney or liver parenchyma or associated immune infiltrate in these organs (not depicted).

To confirm the consistency of our findings, we tested whether DCs also exacerbated pancreatitis in a model of endogenous DC expansion using Flt3L (Fms-like tyrosine kinase-3 ligand; Maraskovsky et al., 1996). Mice treated with Flt3L for 10 d developed expansion of pancreatic DC populations between days 4 and 15 (Fig. 7 A). Inflammatory monocyte populations were not significantly expanded (Fig. 7 B). Moreover, treatment with Flt3L and simultaneous challenge with caerulein resulted in exacerbated acinar destruction, fibrosis, and inflammation (Fig. 7, C and D), suggesting that the effects of DC expansion in pancreatitis are not model specific.

In addition to the fibroinflammatory changes, a conspicuous phenotypic finding observed in pancreatitis associated with DC transfer is the widespread development of early PanIN lesions. Overall, ~50% of ducts were classified as PanINs in C+DC pancreata (Fig. 8, A and B). Affected ducts in C+DC-treated mice stained positively for Alcian blue (Fig. 8 C). Pancreata of control animals, including mice receiving DCs alone or caerulein alone, did not exhibit PanIN lesions after 3 wk of treatment. Furthermore, pancreata from C+DC-treated animals had a markedly high fraction of $Ki67^+$ proliferating epithelial cells compared with controls (Fig. 8 D).

DCs accelerate the growth of pancreatic tumors

Prolonged duration of C+DC administration to WT mice for 3 mo resulted in greater fibrodysplastic obliteration of the pancreatic parenchyma and more diffuse PanIN lesions but not invasive carcinoma (Fig. 8 E). However, DCs markedly accelerated malignant transformation when transferred for

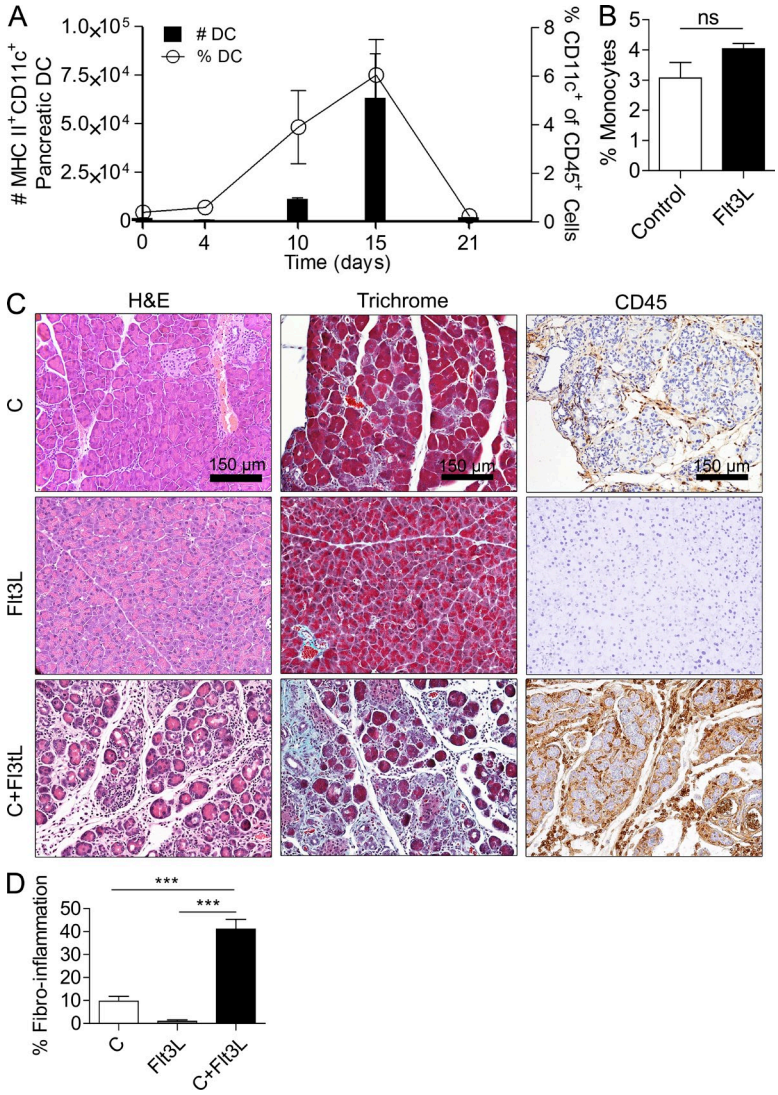

Figure 7. Flt3L treatment exacerbates pancreatitis. (A) The time course of DC expansion in the pancreas of Flt3L-treated WT mice is shown. Both the total number of pancreatic DCs and their fraction among pancreatic leukocytes are indicated. Data are based on a mean of four mice per time point. (B) The fraction of inflammatory monocytes in the pancreata of Flt3L-treated mice and controls was calculated. Day 15 data are shown. (C and D) Mice treated with Flt3L alone, caerulein alone, or caerulein + Flt3L were stained with H&E, Gomori's Trichrome, and anti-CD45. (D) Fibroinflammatory area was quantified by examining 10 HPFs per mouse (five mice per group; ***, $P < 0.001$). Error bars indicate standard error of the mean.

4 wk to p48Cre;Kras^{G12D} mice (Fig. 8, F and G). Furthermore, protein analysis revealed that DC transfer resulted in altered pancreatic expression of numerous cell cycle regulatory and tumor suppressor genes including up-regulated expression of p21, p27, p-p27, p53, and Rb (Fig. 8 H). Moreover, consistent with our previous data (Fig. 4 B), adoptive transfer of DCs derived from MyD88$^{-/-}$ mice resulted in significantly more accelerated tumorigenesis (Fig. 8, F and G). We further tested the protumorigenic capacity of DCs in an orthotopic model. Cohorts of WT mice were challenged with intrapancreatic KRas^{G12D} PDECs and then sacrificed 6 wk later. In parallel, selected mice received thrice weekly DC adoptive transfer beginning in week 2. DCs again induced a threefold accelerated growth rate of pancreatic lesions (Fig. 8 I). The relative distribution of epithelia and stroma was similar in both the control and DC adoptive transfer groups (Fig. 8 J).

DCs mediate effects of MyD88 inhibition in pancreatic disease

To further investigate the augmented proinflammatory and transformative effects of MyD88 inhibition in DCs, we transferred DCs from MyD88$^{-/-}$ mice to WT mice undergoing caerulein pancreatitis. As predicted, MyD88$^{-/-}$ DC transfer worsened pancreatitis (Fig. 9 A) and PanIN formation (Fig. 9 B) to a greater extent than WT DC transfer. Endocrine and exocrine pancreata were almost entirely replaced by collagen after MyD88$^{-/-}$ DC transfer, and >70% of ducts were PanINs. In addition, transfer of MyD88$^{-/-}$ DCs resulted in an approximately twofold increase in CD4$^+$ T cell recruitment compared with transfer of WT DCs (Fig. 9 C). Collectively, these data support our findings using CD11c-Cre MyD88 Floxed$^{+/+}$ mice (Fig. 4, A–D) and together suggest that DCs are sufficient to induce the exacerbated inflammation and dysplasia observed in the MyD88-deficient pancreata.

The DC–Th2 axis mediates exacerbated pancreatitis and transformation

Consistent with our hypothesis that suggests that the DC–CD4 axis can mediate pancreatic inflammation and transformation, we found that CD4$^+$ T cell–deficient mice were protected from the effects of DC transfer in chronic pancreatitis (Fig. 9, D and E). Conversely, the absence of CD8$^+$ T cells, B cells, neutrophils, and monocyte depletion or TNF blockade did not protect C+DC-treated mice (Fig. 9, D and E). Furthermore, in our pancreatic cancer model, CD4$^+$ T cell depletion protected p48Cre;Kras^{G12D} mice adoptively transferred with DCs from developing accelerated carcinogenesis (Fig. 9 F). CD4$^+$ T cell depletion had similarly protective effects after transfer of MyD88$^{-/-}$ DCs (not depicted).

In line with the observations that CD4$^+$ T cells are the critical effectors in DC-mediated pancreatic inflammation and transformation, we found that the number of intrapancreatic CD4$^+$ T cells and CD4/CD8 T cell ratio were markedly increased in mice adoptively transferred with DCs (Fig. 10, A and B). Furthermore, intrapancreatic CD4$^+$ T cells in DC-treated mice exhibited a strong Th2 differentiation (Fig. 10 C). These effects were accentuated by transfer of MyD88$^{-/-}$ DCs (Fig. 10, A–C). In addition to the significant lack of intrapancreatic Th1 and Th17 differentiation, the fraction of intrapancreatic CD4$^+$CD25$^+$Foxp3$^+$ regulatory T cells (T_{reg} cells) was

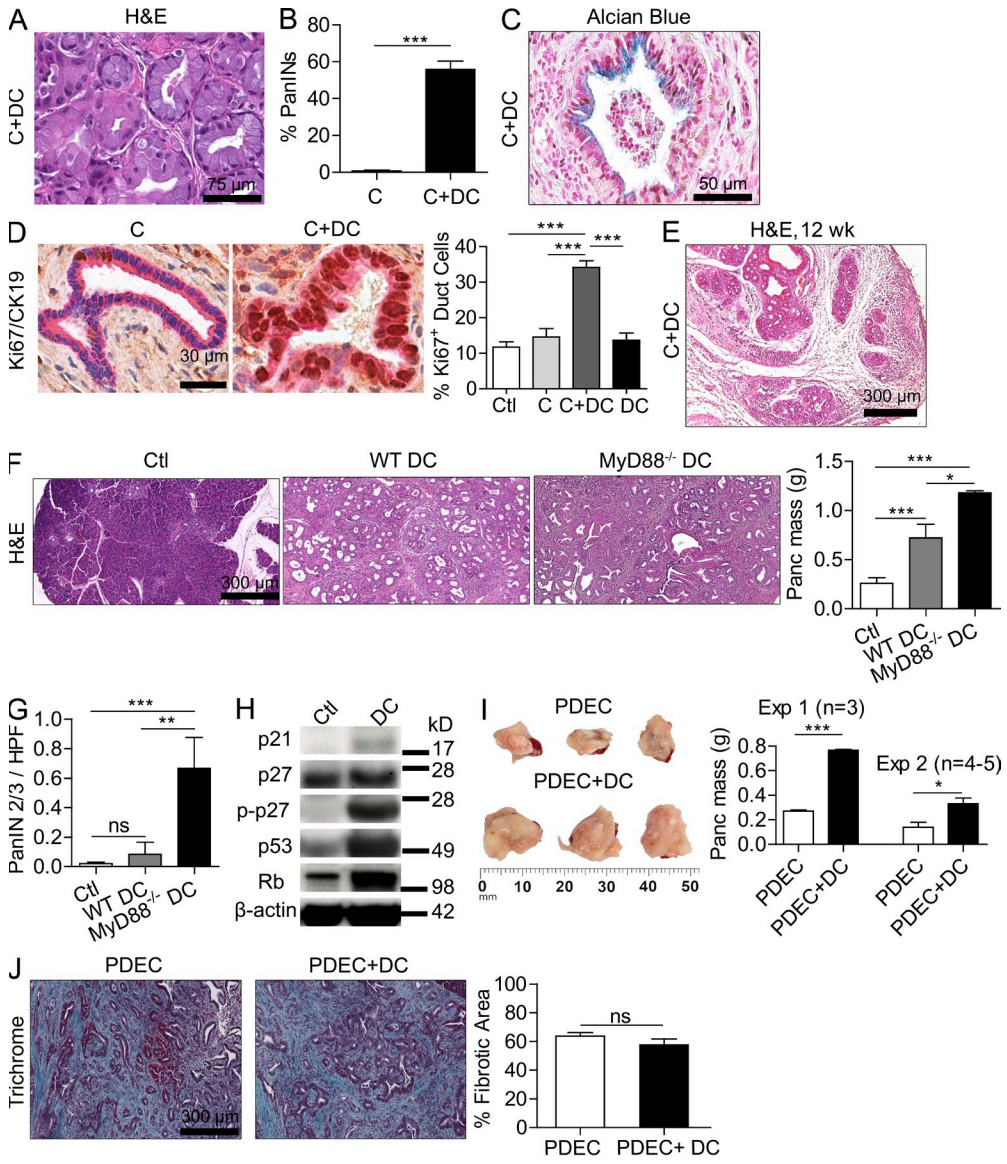

Figure 8. DCs promote the transition from chronic pancreatitis to ductal dysplasia and accelerate the growth rate of pancreatic tumors. (A and B) 4-wk-old WT mice were treated with C or C+DCs for 3 wk. Representative H&E-stained section from C+DC-treated pancreata is shown. The fraction of pancreatic ducts in C or C+DC mice exhibiting PanIN lesions was quantified by examining pancreata from >15 mice per group. (C) Representative paraffin-embedded section of pancreata from mice treated with C+DCs and stained with Alcian blue is shown. (D) Pancreata from mice treated with C or C+DCs were stained for CK19 (pink) and Ki67 (brown), and the fraction of $Ki67^+$ ductal cells was quantified for each treatment group. (E) Representative H&E-stained image of pancreas from a mouse treated for 12 wk with C+DCs. (F and G) 4-wk-old p48Cre;$Kras^{G12D}$ mice were adoptively transferred with DCs derived from WT or $MyD88^{-/-}$ mice thrice weekly for 5 wk before sacrifice (n = 5/group). Representative H&E-stained sections are shown, pancreata were weighed, and the fraction of PanIN 2/3 ducts per HPF was determined (G). (H) Lysate from pancreata of mice adoptively transferred with WT DCs or saline was tested for expression of p21, p27, p-p27, p53, and Rb by Western blotting. (I) Mice were challenged with 3×10^6 (experiment 1) or 10^6 (experiment 2) $KRas^{G12D}$ PDECs. In each experiment, selected mice were adoptively transferred with DCs (10^6) thrice weekly from weeks 2–6. Mice were sacrificed after 6 wk, and pancreatic lesions were weighed. (J) Representative Trichrome-stained paraffin-embedded sections are shown, and the fraction of fibrotic pancreatic area was quantified (*, $P < 0.05$; **, $P < 0.01$; ***, $P < 0.001$). Error bars indicate standard error of the mean.

also markedly reduced in C+DC-treated animals (Fig. 10 D). Similarly, MHC $II^{-/-}$ mice, which are deficient in Th2 signaling, were protected from the effects of DC expansion in pancreatitis, whereas β2-microglobulin$^{-/-}$ mice deficient in $CD8^+$ T cell signaling were not protected (Fig. 10, E and F). Collectively, our data suggest that DC expansion in the injured pancreas increases $CD4^+$ T cell Th2 differentiation, which is required for the organ destructive, fibrotic, inflammatory, and dysplastic effects, and decreases the fraction of other T cell subsets, including T_{reg} cells and $CD8^+$ cells.

We postulated that DCs induce Th2-deviated $CD4^+$ T cells by capturing antigen from the injured pancreas, which

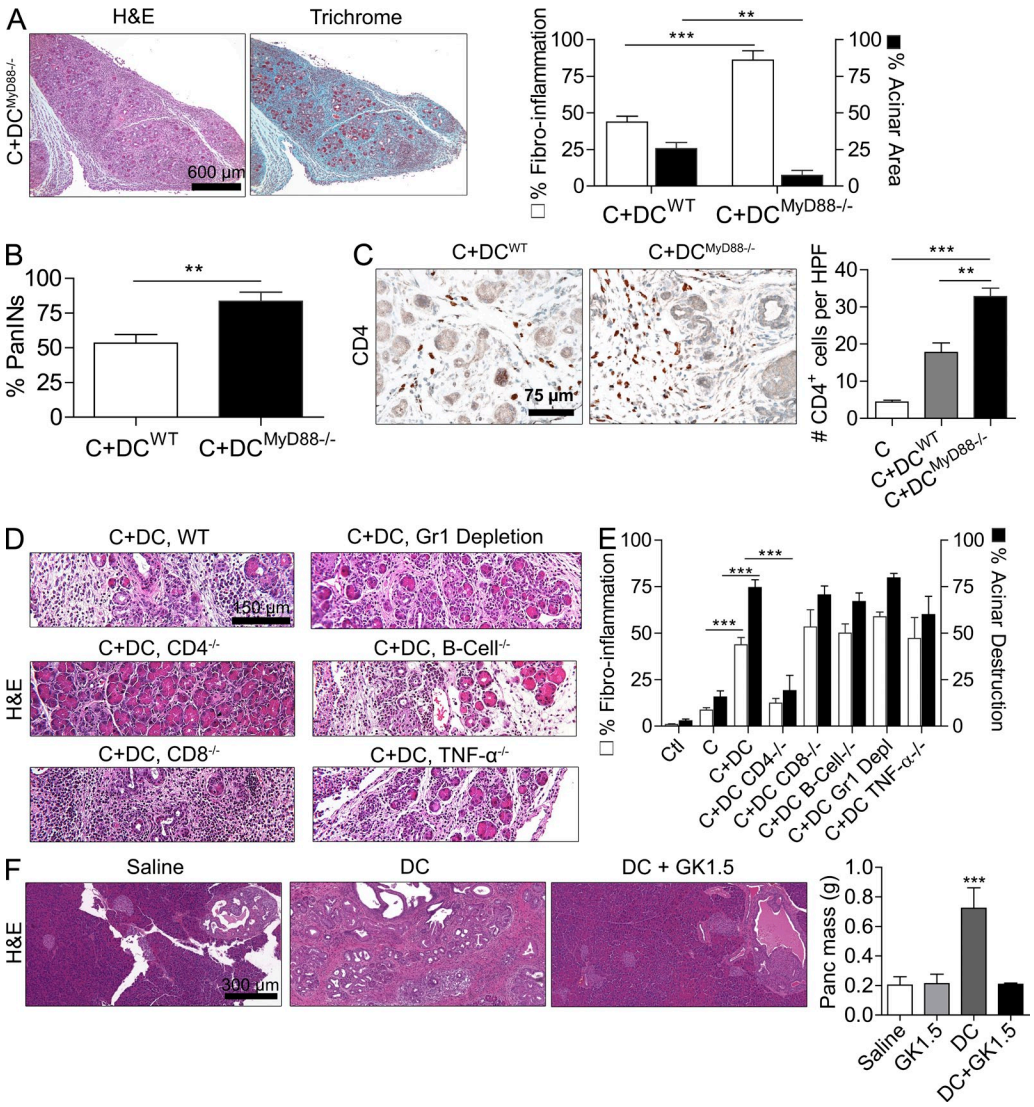

Figure 9. Fibroinflammatory and dysplastic effects of DCs are exaggerated upon MyD88 inhibition and are contingent on CD4+ T cells. (A–C) MyD88$^{-/-}$ or WT DCs were adoptively transferred to WT mice undergoing caerulein-induced chronic pancreatitis. The extent of fibrosis and acinar destruction (A), as well as PanIN formation (B) and size of the CD4+ T cell infiltrate (C) in pancreata of treated animals were determined. Experiments were performed using a mean of five mice per group (**, $P < 0.01$; ***, $P < 0.001$). (D and E) Mice deficient in CD4+ T cells, CD8+ T cells, B cells, Gr1+ inflammatory monocytes and neutrophils, or TNF production were induced to develop chronic pancreatitis in the context of DC overexpansion. Pancreatic effacement and fibroinflammatory changes were quantified for each group by examining 10 HPFs per slide ($n = 4$–6 mice/experimental group; ***, $P < 0.001$). (F) 4-wk-old p48Cre;Kras^{G12D} mice were adoptively transferred with DCs or administered saline for 5 wk. Selected cohorts were additionally treated with GK1.5 to deplete CD4+ T cells. Pancreas weights were measured ($n = 4$ mice/experimental group; ***, $P < 0.001$). Error bars indicate standard error of the mean.

they present to naive T cells, thereby generating antigen-restricted effector cells. To test whether these effectors are specific to pancreatic antigen, CD4+ T cells from the pancreata of C+DC-treated WT mice were purified and cultured for 5 d with either mock-loaded DCs or DCs loaded with lysate from digested pancreata. CD4+ T cells co-cultured with pancreatic lysate–pulsed DCs exhibited increased activation compared with controls, implying pancreas-directed specificity (Fig. 10 G). Furthermore, transfer of CD4+ T cells from C+DC-treated WT mice to p48Cre;Kras^{G12D} mice markedly accelerated pancreatic cancer development, whereas CD4+ T cell transfer from control mice did not have tumor-promoting effects (Fig. 10, H and I).

DISCUSSION

Pancreatic cancer is a devastating disease with very few effective treatment options as <5% of patients achieve cure (Vincent et al., 2011). Recent evidence suggests that rather than being a dormant component, pancreatic fibroinflammatory stroma impacts malignant transformation and disease progression.

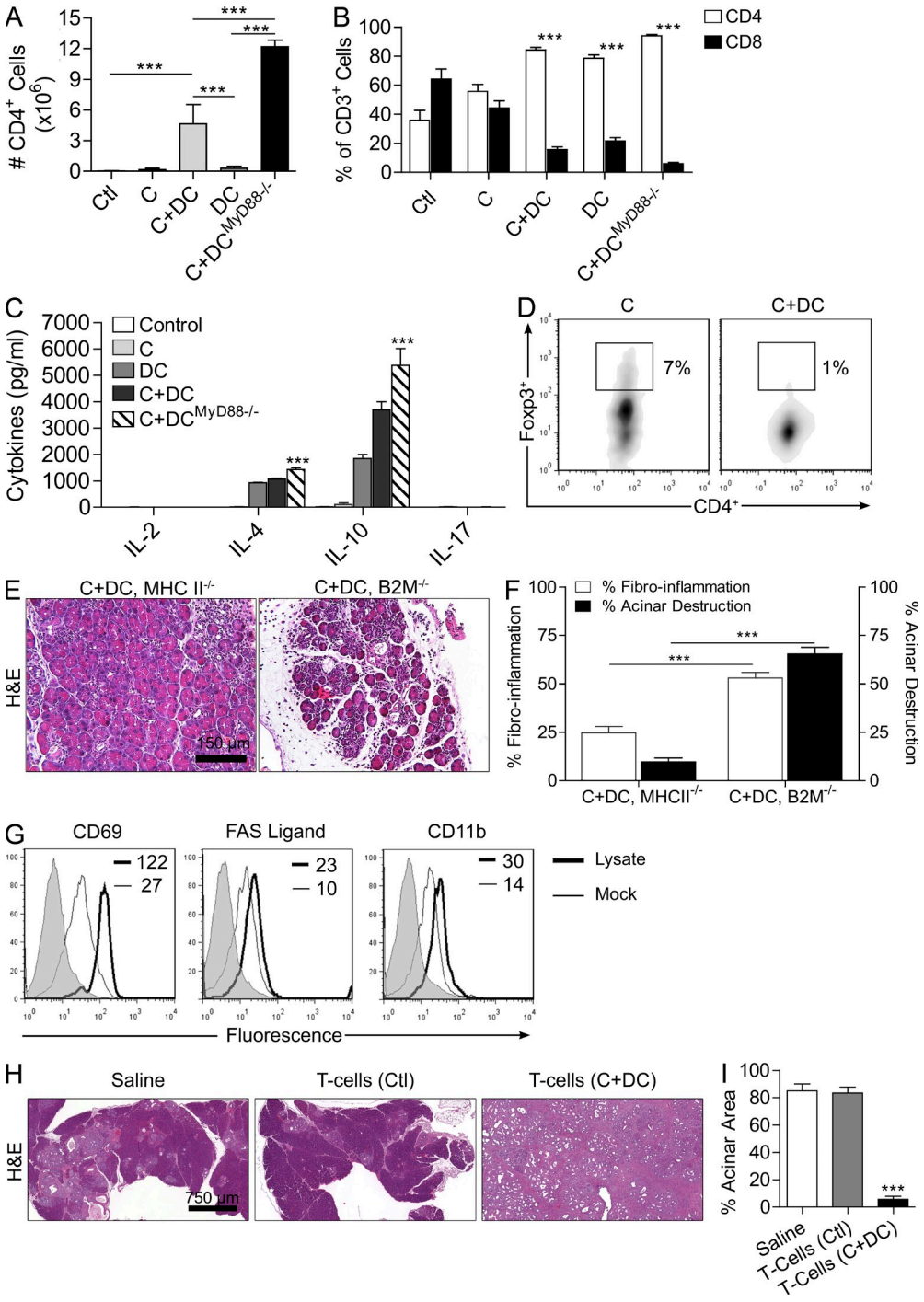

Figure 10. DCs exacerbate pancreatic disease by inducing antigen-restricted Th2 cells. (A and B) The total number of $CD4^+$ cells in the pancreata of mice treated with $C+DC^{WT}$, $C+DC^{MyD88-/-}$, and controls (A) and the fraction of intrapancreatic $CD4^+$ or $CD8^+$ T cells among all $CD3^+$ cells (B) were measured by flow cytometry (***, $P < 0.001$). (C) $CD4^+$ T cell differentiation in the pancreas of mice treated with $C+DC^{WT}$, $C+DC^{MyD88-/-}$, and controls was determined by measuring their production of Th1, Th2, and Th17 cytokines after FACS sorting. (D) The fraction of intrapancreatic T_{reg} cells was determined by gating on $CD45^+CD25^+$ leukocytes and cross staining for CD4 and Foxp3. In vitro assays were repeated three times with similar results. (E and F) MHC $II^{-/-}$ and β2-microglobulin$^{-/-}$ mice treated with caerulein were recipients of DC transfer. A mean of four mice per group was used in these experiments (***, $P < 0.001$). (G) To determine the pancreatic antigen specificity of effector T cells, FACS-sorted pancreas-infiltrating $CD4^+$ T cells from WT C+DC-treated mice were cultured with pancreatic lysate– or mock-pulsed DCs. $CD4^+$ T cell activation was then determined by their expression of CD69, FAS ligand, and CD11b. Gray histograms represent isotype control. Median fluorescent indexes are shown for each group. Experiments were repeated three times with similar results. (H and I) p48Cre;$Kras^{G12D}$ mice were adoptively transferred for 5 wk with $CD4^+$ T cells derived from control and C+DC-treated mice ($n = 3$/group). Representative H&E-stained sections and images of pancreata are shown (H), and the fraction of pancreatic area with preserved acinar architecture was measured (I; ***, $P < 0.001$). Error bars indicate standard error of the mean.

In particular, by releasing nutrient growth factors into the nescient tumor microenvironment, such as insulin-like growth factor and PDGF, the stromal component of pancreatic cancer has been closely linked to carcinogenesis as well as tumor growth and invasiveness (Wang et al., 2007; Mantovani et al., 2010). We postulated that TLR4 may regulate stromal inflammation as it has previously been implicated in benign pancreatic disease (Sharif et al., 2009). Our related findings that TLR4 is increased in expression on leukocytes within the tumor microenvironment in humans and mice, that TLR4 ligands such as HMGB-1 and S100A9 are rife within the tumor microenvironment, and that TLR4 ligation accelerates carcinogenesis in mice lends insight into the mechanism of regulation of pancreatic tumor progression by the inflammatory stroma. We further show that TLR4 signaling via the MyD88-independent TRIF pathway modulates pancreatic carcinogenesis as targeting TLR4 or TRIF prevents cancer progression in at risk pancreata. These data suggest that testing clinical-grade TLR4 or TRIF inhibitors in pancreatic cancer would be appropriate (Barrat and Coffman, 2008). Our findings also suggest that there may possibly be a role for endogenous LPS derived from gut bacteria in modulating pancreatic carcinogenesis. Indeed, a role for the microbiome in carcinogenesis is rapidly emerging in colon cancer and other malignancies (Ahn et al., 2012; Dapito et al., 2012), and our data suggest mechanistic plausibility for its possible influence on pancreatic oncogenesis. However, definitive linkage of pancreatic cancer development to the host microbiome via TLR4 requires more exact investigation.

An equally compelling discovery in this study is that MyD88 blockade vigorously accelerates pancreatic fibroinflammation as well as carcinogenesis. Most notably, MyD88 blockade resulted in invasive pancreatic adenocarcinoma within 3 wk in p48Cre;$Kras^{G12D}$ mice treated with caerulein compared with the development of early PanIN lesions in age-matched mice with intact MyD88 signaling. Moreover, malignant epithelial cells in MyD88-deficient mice exhibited altered expression of p53 in the absence of an endogenous p53 mutation. Overexpression of p53 in pancreatic cancer has been linked to peritumoral inflammation and is associated with an aggressive oncogenic phenotype (Carrière et al., 2011). Our findings contrast with studies linking MyD88 to inflammation and carcinogenesis (Gasse et al., 2007; Rakoff-Nahoum and Medzhitov, 2007; Swann et al., 2008; Coste et al., 2010). For example, Rakoff-Nahoum and Medzhitov (2007) crossed $APC^{min/+}$ mice, which carry a germline mutation in the *Apc* tumor suppressor gene, with MyD88-deficient mice and found that the absence of MyD88 signaling resulted in a decreased number of intestinal polyps and substantially improved survival. Recently, Coste et al. (2010) also showed that MyD88 plays a cell-autonomous role in Ras-mediated transformation in mouse and human tissues. The proinflammatory and carcinogenic effects of MyD88 inhibition in the pancreas are unlikely related to unremitting TRIF signaling as combined TRIF and MyD88 blockade nonetheless resulted in severe pancreatic disease. Rather, the resolution to our ostensibly paradoxical finding lies in the fact that in the presence of MyD88 blockade, DCs preferentially induce Th2 polarization (Kaisho et al., 2002; Kapsenberg, 2003; Chen et al., 2010), which, in pancreatic disease, compensates for the inability to produce generalized inflammation via NF-κB (Fig. S1). We demonstrate that DCs are the causal cellular component responsible for exacerbated chronic pancreatitis and neoplasia upon MyD88 blockade by using DC adoptive transfer experiments using $MyD88^{-/-}$ DCs and by examining CD11c-Cre MyD88 $Floxed^{+/+}$ mice, which are deficient in MyD88 signaling exclusively within $CD11c^+$ cells.

The observation that DCs exacerbate pancreatic pathology through the activation and expansion of pancreas-restricted Th2-deviated $CD4^+$ T cell population was supported by the protection offered in MHC $II^{-/-}$ mice compared with β2-$microglobulin^{-/-}$ mice, our finding that $CD4^+$ T cells derived from C+DC pancreata could accelerate tumorigenesis when transferred to p48Cre;$Kras^{G12D}$ animals, and that depletion of Th2-deviated $CD4^+$ T cells protects against the proinflammatory and tumorigenic effects of DC adoptive transfer or MyD88 blockade. Furthermore, given the intrapancreatic expansion of Th2 cells upon DC transfer, and suppression of $CD8^+$, Th1, Th17, and T_{reg} cell differentiation, and our observation that these effector T cells recognize pancreatic antigen, a logical hypothesis governing the DC–Th2 axis in pancreatic carcinogenesis is that infiltrating DCs capture pancreatic antigen and induce antigen-restricted Th2 $CD4^+$ T cell differentiation, which then serve as the effector cell mediating cellular injury and inflammation required for stromal activation and neoplastic transition. Our discovery of the importance of Th2 polarization in pancreatic disease corresponds with recent studies that have shown an association between Th2-mediated inflammation and neoplastic development in patients with melanoma and in experimental models of colon carcinogenesis (Osawa et al., 2006; Nevala et al., 2009). Human pancreatic cancer is also marked by an extensive peritumoral Th2 infiltration, which is associated with reduced survival (De Monte et al., 2011). The current data suggest that DCs are sufficient to induce accelerated pancreatic tumorigenesis via induction of pancreatic antigen-restricted Th2-deviated $CD4^+$ T cells. However, it is notable that $CD4^+$ T cell depletion did not rescue p48Cre;$Kras^{G12D}$ mice outside of the context of MyD88 blockade (Fig. 4 D), suggesting that alternate protumorigenic mechanisms, rather than DC-$CD4^+$ T cell activity, may be primary in pancreata of p48Cre;$Kras^{G12D}$ mice with intact MyD88 signaling pathways.

The paradigm linking inflammation and inflammatory cells to carcinogenesis has been gaining consistent momentum in the scientific literature (Colotta et al., 2009; Mantovani et al., 2010). A heightened inflammatory milieu provides a continuous supply of cytokines and growth factors that can affect biological processes responsible for maintaining cellular homeostasis, leading to genetic instability and an increased risk of carcinogenesis (Greer and Whitcomb, 2009). Our experiments revealed a robust, pancreas-specific expansion of DC populations in animals subject to both benign and malignant pancreatic disease and in human pancreatic cancer tissue.

We show that DC expansion within the inflamed pancreas leads to the formation of early PanIN lesions with high proliferative rates. Furthermore, DCs accelerate pancreatic tumor growth and are sufficient to induce altered expression of numerous cell cycle regulatory genes and tumor suppressor genes. DCs have been considered a potent tool in nature's defense against carcinogenesis and tumor progression as DCs avidly capture tumor antigen in vivo and initiate both adaptive and innate antitumor immune responses (O'Neill et al., 2004; Petersen et al., 2010). Conversely, we describe a deleterious role for DCs as potent protumorigenic agents in the pancreatic stroma. The concept of DCs as protumorigenic is consistent with recent studies showing that thymic stromal lymphopoietin engenders the growth of human breast cancer by promoting Th2 inflammation via $OX40L^+$ DCs (Ito et al., 2005; Liu et al., 2011). This protumorigenic capacity of DCs might explain, in part, the reason DC immunotherapy and vaccine regimens have shown limited clinical efficacy in the treatment of human cancers (Palucka et al., 2009; Robson et al., 2010). Moreover, this work could provide a rationale for experimental therapeutic strategies aimed at targeting DCs in individuals with chronic pancreatitis who are at greatest risk for transformation.

The current study must be viewed in the context of our very recent study, which found that DCs have a parallel protective role in acute pancreatic inflammation (Bedrosian et al., 2011). That is, we found that DC depletion in acute pancreatitis, rather than mitigating injury, results in complete exocrine organ necrosis. We showed that the mechanism for the pancreatic destruction upon DC depletion may be related to their critical role in the clearance of apoptotic cells and necrotic debris during the regeneration phase of pancreatitis. Conversely, in the context of DC depletion, there is a severe deficiency in the clearance of cellular debris and a parallel rise in sterile inflammation within the pancreas, resulting in acinar organ necrosis with sparing of the islets (Bedrosian et al., 2011). Thus, within the same organ and in one disease, our studies show that DCs can have dual opposing effects. These are the first findings of parallel pro-fibroinflammatory and dysplastic as well as protective roles for DCs within the context of organ-specific inflammation and may have implications to understanding the complex role of DCs in other immune-based diseases.

MATERIALS AND METHODS

Animals and procedures. Male C57BL/6 (H-2Kb) were purchased from Taconic and bred in-house. Transgenic mice deficient in CD4 T cells (B6.129S2-*Cd4*^{tm1Mak}/J), CD8 T cells (B6.129S2-*Cd8a*^{tm1Mak}/J), B cells (B6.129S2-*Igh-6*^{tm1Cgn}/J), MHC II (B6.129S2-*C2ta*^{tm1Ccum}/J), β2-microglobulin (B6.129P2-B2m^{tm1Unc}/J), TNF (B6.129S-*Tnf* ^{tm1Gkl}/J), TRIF (C57BL/6J-*Ticam1*^{Lps2}/J), and TLR4 (B6.B10ScN-*Tlr4*$^{lps-del}$/JthJ) were purchased from the Jackson Laboratory. p48Cre;Kras^{G12D} mice, which develop pancreatic neoplasia endogenously by expressing a single mutant *Kras* allele in progenitor cells of the pancreas (gift of D. Tuveson, Cambridge Research Institute, Cambridge, England, UK), were generated by crossing LSL-Kras^{G12D} mice with p48-Cre mice, which express Cre recombinase from a pancreatic progenitor-specific promoter (Hingorani et al., 2003). MyD88$^{-/-}$ mice were a gift of D. Levy (New York University School of Medicine, New York, NY). CD11c-Cre MyD88 Floxed$^{+/+}$ mice, which are deficient in MyD88 exclusively within $CD11c^+$ cells, were generated by breeding B6.129P2(SJL)-*Myd88*^{tm1Defr}/J mice with B6.Cg-Tg(Itgax-cre)1-1Reiz/J (The Jackson Laboratory) as reported previously (Hou et al., 2008). Bone marrow chimeric animals were created by irradiating 2-mo-old mice (100 Gy) followed by i.v. bone marrow transfer (10^7 cells) from nonirradiated donors as we have described previously (Bedrosian et al., 2011). Chimeric mice were used in experiments 7 wk later. To accelerate carcinogenesis in p48Cre;Kras^{G12D} mice, two doses of caerulein (50 μg/kg; Sigma-Aldrich) were administered over 48 h as described previously with modifications, and mice were sacrificed at 3 wk (Carrière et al., 2009). Animals were housed in a clean vivarium and fed standard mouse chow. Animal procedures were approved by the New York University School of Medicine Institutional Animal Care and Use Committee.

Cellular isolation, culture, and analysis. Bone marrow–derived DCs we generated as described previously (Miller et al., 2002). In brief, bone marrow aspirates were cultured for 8 d in complete RPMI supplemented with 20 ng/ml murine GM-CSF. Pancreatic and splenic mononuclear cells were isolated by mechanical and chemical digestion using Collagenase IV (Sigma-Aldrich). For selected experiments, $CD4^+$ T cells were purified from suspensions of pancreatic mononuclear cells using the MoFlo Cell Sorter (Beckman Coulter) and cultured with plate-bound anti-CD3. Cell culture supernatant was assayed in a cytometric bead array (BD).

In vivo models. Chronic pancreatitis was induced using seven consecutive hourly i.p. injections of caerulein (50 μg/kg; Sigma-Aldrich) thrice weekly for 3–12 wk. In animals adoptively transferred with DCs, 10^6 bone marrow–derived DCs were administered i.p. thrice weekly. In selected animals, 10 μg Flt3L was administered i.p. for 10 d. In parallel, caerulein was administered thrice weekly for 2 wk starting on day 4 of Flt3L administration. For $CD4^+$ T cell adoptive transfer experiments, 2×10^5 pancreatic $CD4^+$ T cells were purified and transferred administered i.p. thrice weekly for 5 wk. To establish orthotopic pancreatic lesions, we grafted PDECs harboring oncogenic KRas^{G12D} by direct intrapancreatic injection via laparotomy as we have described previously (Agbunag et al., 2006; Pylayeva-Gupta et al., 2012). Mice were sacrificed 6 wk after PDEC transfer. To deplete $Gr1^+$ cells or $CD4^+$ T cells, respectively, RB6-8C5 or GK1.5 was used as described previously (Connolly et al., 2010; Monoclonal Antibody Core Facility, Memorial Sloan-Kettering Cancer Center). MyD88 inhibitory peptide or control peptide (200 μg; InvivoGen) was administered i.p. thrice weekly in selected experiments. NF-κB blockade was accomplished using the cell-permeable NEMO binding domain inhibitor (1 mg/kg/day; EMD Millipore). MAP kinase blockade was accomplished using PD98059 (2.5 mg/kg/day; InvivoGen). TLR4 and TRIF blockade was accomplished using a TLR4 inhibitory peptide (IMG-2011A; 100 μg thrice weekly; Imgenex) or an inhibitor of the TRIF adaptor protein (Pepinh-TRIF; 150 μg thrice weekly; InvivoGen), respectively. In selected experiments, mice were treated with 5 μg TLR4 ligand LPS or 80 μg TLR3 ligand Poly I:C thrice weekly (both InvivoGen). The novel immune modulator VAG539 (30 mg/kg/day; Novartis) was administered via oral gavage (Hellerbrand et al., 1996; Creusot et al., 2009). Serum levels of glucose and lipase were measured using an AU400 Chemistry Analyzer (Olympus).

Western blotting. For immunoblotting assays, cell lysates were prepared from whole pancreata or Raji lymphoma cells. For our human experiments, proteins were also isolated from human pancreatic duct fluid harvested at surgery from patients undergoing pancreatic resection. Total protein was determined by the Lowry assay, and lysates were equiloaded onto a 10% polyacrylamide gel (30% acrylamide/Bis solution, 37.5:1, 2.6% C). Proteins were then electrotransferred to a polyvinylidene difluoride membrane at 90 V for 90 min. Subsequently, the polyvinylidene difluoride was immunoblotted using antibodies directed against pIRF3 (Cell Signaling Technology), HMGB-1, S100A9, IRAK, pIRAK, p21, p27, p-p27, p53, Rb, and β-actin (Santa Cruz Biotechnology, Inc.). Levels of TLR4 agonists in pancreatic duct fluid were quantified on HEK-Blue cells (InvivoGen) using fixed quantities of TLR4 ligand (LPS) as controls (Guo et al., 2009).

Flow cytometry. Cell surface marker analysis was performed by flow cytometry using the FACSCalibur (Beckman Coulter) after incubating 5×10^5 cells with 1 µg anti-FcγRIII/II antibody (2.4G2, Fc block; Monoclonal Antibody Core Facility, Memorial Sloan-Kettering Cancer Center) and then labeling with 1 µg FITC-, PE-, PerCP-, or APC-conjugated antibodies directed against MHC II ($I\text{-}A^b$), B220 (RA3-6B2), CD3ε (17A2), CD4 (RM4-5) CD8α (53-6.7), CD11b (M1/70), CD11c (HL3), CD25 (PC61.5), CD40 (HM40-3), CD45.2 (104), CD69 (H1.2F3), CD86 (GL1), F/480 (BM8), Foxp3 (FJK-16s), FAS Ligand (MFL3), NK1.1 (PK136), and Gr1 (RB6-8C5; all BD, eBioscience, or BioLegend). Pancreatic mononuclear cells were also stained for TLR4 (Imgenex). Dead cells were excluded by staining with 7-amino-actinomycin D (BD).

Histology, immunohistochemistry, and microscopy. For histological analysis, paraffin-embedded or frozen sections were stained with hematoxylin and eosin (H&E), Gomori's Trichrome, Alcian blue, or Picric acid–Sirius red. In addition, immunohistochemistry was performed using antibodies directed against CD3 (Invitrogen), CD4 (Abbiotec), p53 (Novocastra), CK19 (Developmental Studies Hybridoma Bank), Desmin (Sigma-Aldrich), α-SMA (Novus Biologicals), TLR4 (Imgenex), amylase (Sigma-Aldrich), CD11c, DC-SIGN, CD1a (BD), CD123, and insulin (Abcam). Photographs were taken using a DM2M microscope (Leica) and a digital camera (Optronics). Fluorescent images were captured on an Axiovert 200M fluorescence microscope (Carl Zeiss). Ductal dysplasia was identified and graded in a blinded manner according to established criteria (Hingorani et al., 2003; Hruban et al., 2004). In brief, in PanIN I lesions, the normal cuboidal PDECs transition to columnar architecture. PanIN II lesions are associated with additional nuclear abnormalities such as loss of polarity. PanIN III lesions, or in situ carcinoma, show cribriforming, budding off of cells, and luminal necrosis with marked cytological abnormalities, without invasion beyond the basement membrane.

Statistics. Data are presented as mean ± standard error of mean. Statistical significance was determined by the Student's *t* test or the log-rank test using Prism 4 (GraphPad Software). P-values < 0.05 were considered significant.

Online supplemental material. Fig. S1 shows divergent effects of modulating MyD88 and TRIF signaling on pancreatic carcinogenesis. Online supplemental material is available at http://www.jem.org/cgi/content/full/jem.20111706/DC1.

This work was supported in part by grants from the Society of University Surgeons (to G. Miller), the National Pancreas Foundation (to G. Miller), the Irvington Institute Postdoctoral Fellowship Program of the Cancer Research Institute (to Y. Pylayeve-Gupta), and National Institutes of Health Awards CA108573 (to A.B. Frey), CA055360 (to D. Bar-Sagi), DK085278 (to G. Miller), and CA155649 (to G. Miller). The Flow Cytometry and Histology and Immunohistochemistry Core Facilities of the New York University School of Medicine are partially supported by the National Institutes of Health (grant 5 P30CA016087-31).

The authors have no conflicting financial interests.

Submitted: 12 August 2011
Accepted: 27 July 2012

REFERENCES

Agbunag, C., K.E. Lee, S. Buontempo, and D. Bar-Sagi. 2006. Pancreatic duct epithelial cell isolation and cultivation in two-dimensional and three-dimensional culture systems. *Methods Enzymol.* 407:703–710. http://dx.doi.org/10.1016/S0076-6879(05)07055-2

Ahn, J., C.Y. Chen, and R.B. Hayes. 2012. Oral microbiome and oral and gastrointestinal cancer risk. *Cancer Causes Control.* 23:399–404. http://dx.doi.org/10.1007/s10552-011-9892-7

Ammann, R.W., A. Akovbiantz, F. Largiader, and G. Schueler. 1984. Course and outcome of chronic pancreatitis. Longitudinal study of a mixed medical-surgical series of 245 patients. *Gastroenterology.* 86:820–828.

Bantsimba-Malanda, C., J. Marchal-Sommé, D. Goven, O. Freynet, L. Michel, B. Crestani, and P. Soler. 2010. A role for dendritic cells in bleomycin-induced pulmonary fibrosis in mice? *Am. J. Respir. Crit. Care Med.* 182:385–395. http://dx.doi.org/10.1164/rccm.200907-1164OC

Barrat, F.J., and R.L. Coffman. 2008. Development of TLR inhibitors for the treatment of autoimmune diseases. *Immunol. Rev.* 223:271–283. http://dx.doi.org/10.1111/j.1600-065X.2008.00630.x

Bedrosian, A.S., A.H. Nguyen, M. Hackman, M.K. Connolly, A. Malhotra, J. Ibrahim, N.E. Cieza-Rubio, J.R. Henning, R. Barilla, A. Rehman, et al. 2011. Dendritic cells promote pancreatic viability in mice with acute pancreatitis. *Gastroenterology.* 141:1915–1926: e1–e14. http://dx.doi.org/10.1053/j.gastro.2011.07.033

Braganza, J.M., S.H. Lee, R.F. McCloy, and M.J. McMahon. 2011. Chronic pancreatitis. *Lancet.* 377:1184–1197. http://dx.doi.org/10.1016/S0140-6736(10)61852-1

Carrière, C., A.L. Young, J.R. Gunn, D.S. Longnecker, and M. Korc. 2009. Acute pancreatitis markedly accelerates pancreatic cancer progression in mice expressing oncogenic Kras. *Biochem. Biophys. Res. Commun.* 382: 561–565. http://dx.doi.org/10.1016/j.bbrc.2009.03.068

Carrière, C., A.J. Gore, A.M. Norris, J.R. Gunn, A.L. Young, D.S. Longnecker, and M. Korc. 2011. Deletion of Rb accelerates pancreatic carcinogenesis by oncogenic Kras and impairs senescence in premalignant lesions. *Gastroenterology.* 141:1091–1101. http://dx.doi.org/10.1053/j.gastro.2011.05.041

Chen, L., L. Lei, X. Chang, Z. Li, C. Lu, X. Zhang, Y. Wu, I.T. Yeh, and G. Zhong. 2010. Mice deficient in MyD88 Develop a Th2-dominant response and severe pathology in the upper genital tract following *Chlamydia muridarum* infection. *J. Immunol.* 184:2602–2610. http://dx.doi.org/10.4049/jimmunol.0901593

Colotta, F., P. Allavena, A. Sica, C. Garlanda, and A. Mantovani. 2009. Cancer-related inflammation, the seventh hallmark of cancer: links to genetic instability. *Carcinogenesis.* 30:1073–1081. http://dx.doi.org/10.1093/carcin/bgp127

Connolly, M.K., A.S. Bedrosian, J. Mallen-St Clair, A.P. Mitchell, J. Ibrahim, A. Stroud, H.L. Pachter, D. Bar-Sagi, A.B. Frey, and G. Miller. 2009. In liver fibrosis, dendritic cells govern hepatic inflammation in mice via TNF-alpha. *J. Clin. Invest.* 119:3213–3225.

Connolly, M.K., J. Mallen-St Clair, A.S. Bedrosian, A. Malhotra, V. Vera, J. Ibrahim, J. Henning, H.L. Pachter, D. Bar-Sagi, A.B. Frey, and G. Miller. 2010. Distinct populations of metastases-enabling myeloid cells expand in the liver of mice harboring invasive and preinvasive intra-abdominal tumor. *J. Leukoc. Biol.* 87:713–725. http://dx.doi.org/10.1189/jlb.0909607

Connolly, M.K., D. Ayo, A. Malhotra, M. Hackman, A.S. Bedrosian, J. Ibrahim, N.E. Cieza-Rubio, A.H. Nguyen, J.R. Henning, M. Dorvil-Castro, et al. 2011. Dendritic cell depletion exacerbates acetaminophen hepatotoxicity. *Hepatology.* 54:959–968. http://dx.doi.org/10.1002/hep.24429

Coste, I., K. Le Corf, A. Kfoury, I. Hmitou, S. Druillennec, P. Hainaut, A. Eychene, S. Lebecque, and T. Renno. 2010. Dual function of MyD88 in RAS signaling and inflammation, leading to mouse and human cell transformation. *J. Clin. Invest.* 120:3663–3667. http://dx.doi.org/10.1172/JCI42771

Creusot, R.J., S.S. Yaghoubi, P. Chang, J. Chia, C.H. Contag, S.S. Gambhir, and C.G. Fathman. 2009. Lymphoid-tissue-specific homing of bone-marrow-derived dendritic cells. *Blood.* 113:6638–6647. http://dx.doi.org/10.1182/blood-2009-02-204321

Dapito, D.H., A. Mencin, G.Y. Gwak, J.P. Pradere, M.K. Jang, I. Mederacke, J.M. Caviglia, H. Khiabanian, A. Adeyemi, R. Bataller, et al. 2012. Promotion of hepatocellular carcinoma by the intestinal microbiota and TLR4. *Cancer Cell.* 21:504–516. http://dx.doi.org/10.1016/j.ccr.2012.02.007

De Monte, L., M. Reni, E. Tassi, D. Clavenna, I. Papa, H. Recalde, M. Braga, V. Di Carlo, C. Doglioni, and M.P. Protti. 2011. Intratumor T helper type 2 cell infiltrate correlates with cancer-associated fibroblast thymic stromal lymphopoietin production and reduced survival in pancreatic cancer. *J. Exp. Med.* 208:469–478. http://dx.doi.org/10.1084/jem.20101876

Demols, A., O. Le Moine, F. Desalle, E. Quertinmont, J.L. Van Laethem, and J. Devière. 2000. CD4(+)T cells play an important role in acute experimental pancreatitis in mice. *Gastroenterology.* 118:582–590. http://dx.doi.org/10.1016/S0016-5085(00)70265-4

Ding, S.Q., Y. Li, Z.G. Zhou, C. Wang, L. Zhan, and B. Zhou. 2010. Toll-like receptor 4-mediated apoptosis of pancreatic cells in cerulein-induced acute pancreatitis in mice. *HBPD INT.* 9:645–650.

Gasse, P., C. Mary, I. Guenon, N. Noulin, S. Charron, S. Schnyder-Candrian, B. Schnyder, S. Akira, V.F. Quesniaux, V. Lagente, et al. 2007. IL-1R1/MyD88 signaling and the inflammasome are essential in pulmonary inflammation and fibrosis in mice. *J. Clin. Invest.* 117:3786–3799.

Greer, J.B., and D.C. Whitcomb. 2009. Inflammation and pancreatic cancer: an evidence-based review. *Curr. Opin. Pharmacol.* 9:411–418. http://dx.doi.org/10.1016/j.coph.2009.06.011

Guo, J., J. Loke, F. Zheng, F. Hong, S. Yea, M. Fukata, M. Tarocchi, O.T. Abar, H. Huang, J.J. Sninsky, and S.L. Friedman. 2009. Functional linkage of cirrhosis-predictive single nucleotide polymorphisms of Toll-like receptor 4 to hepatic stellate cell responses. *Hepatology.* 49:960–968. http://dx.doi.org/10.1002/hep.22697

Hauben, E., S. Gregori, E. Draghici, B. Migliavacca, S. Olivieri, M. Woisetschläger, and M.G. Roncarolo. 2008. Activation of the aryl hydrocarbon receptor promotes allograft-specific tolerance through direct and dendritic cell-mediated effects on regulatory T cells. *Blood.* 112: 1214–1222. http://dx.doi.org/10.1182/blood-2007-08-109843

Hellerbrand, S.C., S.C. Wang, H. Tsukamoto, D.A. Brenner, and R.A. Rippe. 1996. Expression of intracellular adhesion molecule 1 by activated hepatic stellate cells. *Hepatology.* 24:670–676. http://dx.doi.org/10.1002/hep.510240333

Hingorani, S.R., E.F. Petricoin, A. Maitra, V. Rajapakse, C. King, M.A. Jacobetz, S. Ross, T.P. Conrads, T.D. Veenstra, B.A. Hitt, et al. 2003. Preinvasive and invasive ductal pancreatic cancer and its early detection in the mouse. *Cancer Cell.* 4:437–450. http://dx.doi.org/10.1016/S1535-6108(03)00309-X

Hou, B., B. Reizis, and A.L. DeFranco. 2008. Toll-like receptors activate innate and adaptive immunity by using dendritic cell-intrinsic and -extrinsic mechanisms. *Immunity.* 29:272–282. http://dx.doi.org/10.1016/j.immuni.2008.05.016

Hruban, R.H., K. Takaori, D.S. Klimstra, N.V. Adsay, J. Albores-Saavedra, A.V. Biankin, S.A. Biankin, C. Compton, N. Fukushima, T. Furukawa, et al. 2004. An illustrated consensus on the classification of pancreatic intraepithelial neoplasia and intraductal papillary mucinous neoplasms. *Am. J. Surg. Pathol.* 28:977–987. http://dx.doi.org/10.1097/01.pas.0000126675.59108.80

Ito, T., Y.H. Wang, O. Duramad, T. Hori, G.J. Delespesse, N. Watanabe, F.X. Qin, Z. Yao, W. Cao, and Y.J. Liu. 2005. TSLP-activated dendritic cells induce an inflammatory T helper type 2 cell response through OX40 ligand. *J. Exp. Med.* 202:1213–1223. http://dx.doi.org/10.1084/jem.20051135

Jura, N., H. Archer, and D. Bar-Sagi. 2005. Chronic pancreatitis, pancreatic adenocarcinoma and the black box in-between. *Cell Res.* 15:72–77. http://dx.doi.org/10.1038/sj.cr.7290269

Kaisho, T., K. Hoshino, T. Iwabe, O. Takeuchi, T. Yasui, and S. Akira. 2002. Endotoxin can induce MyD88-deficient dendritic cells to support T(h)2 cell differentiation. *Int. Immunol.* 14:695–700. http://dx.doi.org/10.1093/intimm/dxf039

Kapsenberg, M.L. 2003. Dendritic-cell control of pathogen-driven T-cell polarization. *Nat. Rev. Immunol.* 3:984–993. http://dx.doi.org/10.1038/nri1246

Lankisch, P.G., A. Löhr-Happe, J. Otto, and W. Creutzfeldt. 1993. Natural course in chronic pancreatitis. Pain, exocrine and endocrine pancreatic insufficiency and prognosis of the disease. *Digestion.* 54:148–155. http://dx.doi.org/10.1159/000201029

Liu, T., T.L. Li, F. Zhao, C. Xie, A.M. Liu, X. Chen, C. Song, L. Cheng, and P.C. Yang. 2011. Role of thymic stromal lymphopoietin in the pathogenesis of nasal polyposis. *Am. J. Med. Sci.* 341:40–47. http://dx.doi.org/10.1097/MAJ.0b013e3181f20489

Mantovani, A., C. Garlanda, and P. Allavena. 2010. Molecular pathways and targets in cancer-related inflammation. *Ann. Med.* 42:161–170. http://dx.doi.org/10.3109/07853890903405753

Maraskovsky, E., K. Brasel, M. Teepe, E.R. Roux, S.D. Lyman, K. Shortman, and H.J. McKenna. 1996. Dramatic increase in the numbers of functionally mature dendritic cells in Flt3 ligand-treated mice: multiple dendritic cell subpopulations identified. *J. Exp. Med.* 184: 1953–1962. http://dx.doi.org/10.1084/jem.184.5.1953

Masamune, A., T. Watanabe, K. Kikuta, and T. Shimosegawa. 2009. Roles of pancreatic stellate cells in pancreatic inflammation and fibrosis. *Clin. Gastroenterol. Hepatol.* 7:S48–S54. http://dx.doi.org/10.1016/j.cgh.2009.07.038

Miller, G., S. Lahrs, V.G. Pillarisetty, A.B. Shah, and R.P. DeMatteo. 2002. Adenovirus infection enhances dendritic cell immunostimulatory properties and induces natural killer and T-cell-mediated tumor protection. *Cancer Res.* 62:5260–5266.

Miller, G., S. Lahrs, and R.P. Dematteo. 2003. Overexpression of interleukin-12 enables dendritic cells to activate NK cells and confer systemic antitumor immunity. *FASEB J.* 17:728–730.

Nevala, W.K., C.M. Vachon, A.A. Leontovich, C.G. Scott, M.A. Thompson, and S.N. Markovic; Melanoma Study Group of the Mayo Clinic Cancer Center. 2009. Evidence of systemic Th2-driven chronic inflammation in patients with metastatic melanoma. *Clin. Cancer Res.* 15:1931–1939. http://dx.doi.org/10.1158/1078-0432.CCR-08-1980

O'Neill, D.W., S. Adams, and N. Bhardwaj. 2004. Manipulating dendritic cell biology for the active immunotherapy of cancer. *Blood.* 104: 2235–2246. http://dx.doi.org/10.1182/blood-2003-12-4392

Oiva, J., H. Mustonen, M.L. Kylänpää, L. Kyhälä, K. Kuuliala, S. Siitonen, E. Kemppainen, P. Puolakkainen, and H. Repo. 2010. Acute pancreatitis with organ dysfunction associates with abnormal blood lymphocyte signaling: controlled laboratory study. *Crit. Care.* 14:R207. http://dx.doi.org/10.1186/cc9329

Omary, M.B., A. Lugea, A.W. Lowe, and S.J. Pandol. 2007. The pancreatic stellate cell: a star on the rise in pancreatic diseases. *J. Clin. Invest.* 117:50–59. http://dx.doi.org/10.1172/JCI30082

Osawa, E., A. Nakajima, T. Fujisawa, Y.I. Kawamura, N. Toyama-Sorimachi, H. Nakagama, and T. Dohi. 2006. Predominant T helper type 2-inflammatory responses promote murine colon cancers. *Int. J. Cancer.* 118:2232–2236. http://dx.doi.org/10.1002/ijc.21639

Palucka, K., H. Ueno, J. Fay, and J. Banchereau. 2009. Harnessing dendritic cells to generate cancer vaccines. *Ann. N. Y. Acad. Sci.* 1174:88–98. http://dx.doi.org/10.1111/j.1749-6632.2009.05000.x

Petersen, T.R., N. Dickgreber, and I.F. Hermans. 2010. Tumor antigen presentation by dendritic cells. *Crit. Rev. Immunol.* 30:345–386. http://dx.doi.org/10.1615/CritRevImmunol.v30.i4.30

Pylayeva-Gupta, Y., K.E. Lee, C.H. Hajdu, G. Miller, and D. Bar-Sagi. 2012. Oncogenic Kras-Induced GM-CSF Production Promotes the Development of Pancreatic Neoplasia. *Cancer Cell.* 21:836–847. http://dx.doi.org/10.1016/j.ccr.2012.04.024

Rakoff-Nahoum, S., and R. Medzhitov. 2007. Regulation of spontaneous intestinal tumorigenesis through the adaptor protein MyD88. *Science.* 317:124–127. http://dx.doi.org/10.1126/science.1140488

Ricci, F., S.E. Kern, R.H. Hruban, and C.A. Iacobuzio-Donahue. 2005. Stromal responses to carcinomas of the pancreas: juxtatumoral gene expression conforms to the infiltrating pattern and not the biologic subtype. *Cancer Biol. Ther.* 4:302–307. http://dx.doi.org/10.4161/cbt.4.3.1501

Robson, N.C., S. Hoves, E. Maraskovsky, and M. Schnurr. 2010. Presentation of tumour antigens by dendritic cells and challenges faced. *Curr. Opin. Immunol.* 22:137–144. http://dx.doi.org/10.1016/j.coi.2010.01.002

Sharif, R., R. Dawra, K. Wasiluk, P. Phillips, V. Dudeja, E. Kurt-Jones, R. Finberg, and A. Saluja. 2009. Impact of toll-like receptor 4 on the severity of acute pancreatitis and pancreatitis-associated lung injury in mice. *Gut.* 58:813–819. http://dx.doi.org/10.1136/gut.2008.170423

Swann, J.B., M.D. Vesely, A. Silva, J. Sharkey, S. Akira, R.D. Schreiber, and M.J. Smyth. 2008. Demonstration of inflammation-induced cancer and cancer immunoediting during primary tumorigenesis. *Proc. Natl. Acad. Sci. USA.* 105:652–656. http://dx.doi.org/10.1073/pnas.0708594105

Vaquero, E., I. Gukovsky, V. Zaninovic, A.S. Gukovskaya, and S.J. Pandol. 2001. Localized pancreatic NF-kappaB activation and inflammatory response in taurocholate-induced pancreatitis. *Am. J. Physiol. Gastrointest. Liver Physiol.* 280:G1197–G1208.

Vincent, A., J. Herman, R. Schulick, R.H. Hruban, and M. Goggins. 2011. Pancreatic cancer. *Lancet.* 378:607–620. http://dx.doi.org/10.1016/S0140-6736(10)62307-0

Wang, Z., D. Kong, S. Banerjee, Y. Li, N.V. Adsay, J. Abbruzzese, and F.H. Sarkar. 2007. Down-regulation of platelet-derived growth factor-D inhibits cell growth and angiogenesis through inactivation of Notch-1 and nuclear factor-kappaB signaling. *Cancer Res.* 67:11377–11385. http://dx.doi.org/10.1158/0008-5472.CAN-07-2803

Zhou, X.Y., Z.G. Zhou, J.L. Ding, L. Wang, R. Wang, B. Zhou, J. Gu, X.F. Sun, and Y. Li. 2010. TRAF6 as the key adaptor of TLR4 signaling pathway is involved in acute pancreatitis. *Pancreas.* 39:359–366. http://dx.doi.org/10.1097/MPA.0b013e3181bb9073